Ocean Engineering 279 (2023) 113750

Contents lists available at ScienceDirect

Ocean Engineering

journal homepage: www.elsevier.com/locate/oceaneng

Risk-informed collision avoidance system design for maritime autonomous surface ships

Paul Lee[a,*], Gerasimos Theotokatos[a], Evangelos Boulougouris[a], Victor Bolbot[b]

[a] Maritime Safety Research Centre, Department of Naval Architecture, Ocean & Marine Engineering, University of Strathclyde, 100 Montrose, Glasgow, G4 0LZ, United Kingdom

[b] Research Group on Safe and Efficient Marine and Ship Systems, Department of Mechanical Engineering (Marine Technology), Aalto University, Espoo, Finland

ARTICLE INFO

Handling Editor: Prof. A.I. Incecik

Keywords:
Maritime Autonomous Surface Ship
Collision Avoidance System
Quantitative Fault Tree Analysis
Risk analysis
Risk metrics
Risk-informed design

ABSTRACT

The maritime industry is paving the way towards developing Maritime Autonomous Surface Ships (MASSs) through the adoption of key enabling technologies for safety-critical operations, which are associated with new challenges, especially at their early design phase. This study aims to develop a methodology to conduct the risk-informed design for the Collision Avoidance System (CAS) of MASSs. Pertinent regulatory instruments are reviewed to identify functional and system requirements and develop a baseline CAS configuration at the component level. Quantitative Fault Tree Analysis is performed to derive risk metrics, such as probability of failure, Importance measures, and Minimal Cut Sets, whereas criticality analysis is conducted to recommend risk-reducing measures. A Short Sea Shipping case study is investigated considering four operating modes based on various weather and illumination conditions. Results demonstrate that the developed Fault Tree diagram provides a robust representation of the CAS failure. The most critical components are found to be related to the Intention Communication and Situation Awareness Systems, the redundancy of which leads to 91% reduction of the CAS probability of failure. This study contributes towards the risk-informed design of safety-critical systems required for the development of MASSs.

1. Introduction

1.1. Background

The maritime industry has been paving the way towards the new “Shipping 4.0” era, due to its potential to enhance social, environmental, and economic sustainability, propelled by the rapid development of advanced technologies associated with the 4th Industrial Revolution (Rødseth et al., 2016). Specifically, “Shipping 4.0” is defined as the fully interconnected maritime ecosystem through the extensive use of the Internet of Things, Cloud Computing, Big Data, Artificial Intelligence (AI), and Cyber-Physical Systems (Aiello et al., 2020). The main actors of this new ecosystem are expected to be the autonomous ships, also known as Maritime Autonomous Surface Ships (MASSs). According to the International Maritime Organisation (IMO), a MASS ‘*can operate independently of human interaction*’ with a basic prerequisite of ‘*securing at least the same levels of safety as conventional ships*’ (IMO, 2018b, 2019). However, one of the main barriers and scepticism of implementing MASSs and their key enabling technologies are the safety assurance, especially of those related with safety-critical operations (Wang et al., 2020).

Safe navigation at sea, and primarily the collision avoidance, is deemed to be one of the most challenging safety-critical autonomous operations for MASSs (Rødseth and Tjora, 2014). The nature of the collision avoidance operation is a demanding endeavour of complex multitasking functions. It requires the control of an underactuated ship of large inertia on a dynamically changing liquid medium whilst being exposed to unpredictable external factors, such as waves, currents, and various extreme weather conditions (Wu et al., 2020). Adequate understanding of the manoeuvrability characteristics, traffic scenarios, navigational rules, and emergency scenarios require great amount of cognitive ability and expert knowledge to make safe collision avoidance decisions (Statheros et al., 2008). According to the European Maritime Safety Agency, recent accident statistics among European Union flag ships over 2014–2022 indicated that accidents of navigational nature accounted for 43% of all occurrences with 13% being collision accidents (EMSA, 2021).

Furthermore, the transition from human operators to autonomous

* Corresponding author.
E-mail address: p.lee@strath.ac.uk (P. Lee).

https://doi.org/10.1016/j.oceaneng.2023.113750
Received 16 July 2022; Received in revised form 11 November 2022; Accepted 16 January 2023
Available online 25 April 2023

ones at higher degrees of autonomy (IMO, 2021a) is expected to introduce additional challenges. Despite the potential of eliminating human error that constitutes as high as 94.7% of all collision accidents (Ugurlu and Cicek, 2022), human contribution in accident prevention, mitigation, and management, though not reported, cannot be underestimated (Wróbel et al., 2017, 2018a; Wu et al., 2020). Moreover, systems or equipment failure is already the second most contributing factor to accidents after human factor (EMSA, 2021) and is expected to be more pronounced at higher degrees of autonomy (Veritas, 2019). Finally, the adaptation of autonomous systems to unknown and emergency situations or their failure mechanisms are hard to be predicted a priori (Rausand and Haugen, 2020).

Hence, the adoption of MASSs manifests the need for systematic and comprehensive risk analyses of their safety-critical autonomous systems (Guo et al., 2021), such as the Collision Avoidance System (CAS) (Rausand and Haugen, 2020). The primary role of such analyses is to understand the risk associated with such systems and support the decision-making pertaining to their design, operation, and maintenance (Aven, 2015).

1.2. Literature review

Pertinent studies in the literature primarily focused on qualitatively analysing preliminary hazards associated with MASS design and operation to support risk-informed design during its early development phases. Based on IMO's formal safety assessment methodology (IMO, 2002), (Rødseth and Tjora, 2014; Rødseth and Burmeister, 2015) performed Hazard Identification Analysis through functional decomposition of an unmanned merchant ship to realise a risk-based design approach. (Thieme et al., 2019) conducted Preliminary Hazard Analysis to identify hazards of a small autonomous passenger ship. (Chang et al., 2021) used Failure Modes and Effects Analysis, Evidential Reasoning, and Rule-based Bayesian Network (BN) to semi-quantitatively rank the major hazards associated with MASS.

Several studies investigated the control structure by qualitatively analysing the risk involved in MASS systems. (Banda et al., 2018) presented a general systemic and systematic safety management framework to assure the safety of autonomous ships design. Following this framework, (Banda et al., 2019) conducted systemic and systematic Hazard Analysis using System-Theoretic Process Analysis (STPA) and Expert Judgement to develop an initial safety management strategy through the definition of safety controls. (Wróbel et al., 2018a) and (Wróbel et al., 2018b, 2019) used STPA and Mitigation Potential Analysis to identify inadequate controls and assess the effectiveness of mitigating measures for a remotely controlled ship and an autonomous ship, respectively.

Other studies developed risk models associated with MASS systems and their operation. (Wróbel et al., 2016) conducted Brainstorming and Hazard Analysis of an unmanned ship and developed a BN-based risk model to describe accident root causes leading to failure propagation. (Thieme and Utne, 2017) presented a risk model based on human-autonomy collaboration Bayesian Belief Network (BBN) to assess the performance relationship between human and technical system for autonomous marine systems. (Zhou et al., 2019) developed a model based on Hierarchical Bayesian Inference to calculate the probability of failure of acquiring adequate situation awareness of a remotely controlled ship. (Utne et al., 2020) developed a supervisory risk control model by conducting Hazard Analysis using STPA and BBN to outline an online risk modelling framework for MASS. (Guo et al., 2021) developed a BBN-based model to assess the collision risk of an autonomous ship with other conventional ships.

Some efforts have been put in assessing the risk associated with the operation of MASS by analysing conventional maritime accidents. (Wróbel et al., 2017) employed What-If Analysis, Human Factors Analysis, Marine Accidents Taxonomy, and Consequences Check to assess the potential impact on reported conventional accidents should the ships were MASSs. (Wu et al., 2020) conducted a similar study following a Hybrid Causal Logic (HCL) methodology that consists of Event Sequence Diagrams, Fault Trees (FTs), and BNs to investigate the probability of collision accidents in various manned and MASS scenarios. (Zhang et al., 2022) employed HCL to investigate the probability of accident of a remotely controlled ship. (Chou et al., 2022) integrated historical marine accident data and Expert Judgment to qualitatively and quantitatively estimate risks associated with the MASS navigation.

The review of the pertinent studies indicates that most studies were limited to qualitative risk analyses, while using some semi-quantitative methods based on expert knowledge. Moreover, most studies employed risk analyses for MASS design and operation, whilst scant research has been conducted for its safety-critical autonomous systems, such as the CAS at a low level of abstraction. (Zhou et al., 2019) quantified the probability of losing adequate situation awareness that was limited to a qualitative safety control structure. (Guo et al., 2021) quantified the probability of collision, whilst considering only a limited number of obstacle detection, decision, and propulsion systems and using some assigned probabilities based on expert opinion. (Wu et al., 2020) investigated a limited number of situation awareness components to derive quantitative results by qualitatively adjusting the probabilities of the risk influencing factors. (Zhang et al., 2022) quantified the probability of contact due to perception, decision-making, and power plant failures, but only the power and propulsion systems were analysed in detail.

The preceding literature review identified the following research gaps.

a. Quantitative risk analysis of a complete CAS at the component level has not been reported.
b. The CAS design for MASSs has not been investigated in detail.

1.3. Aim & contributions

The aim of this study is to develop a methodology to conduct the risk-informed CAS design for MASSs. The main contributions of this study are as follows.

a. A systematic approach is provided to derive a complete baseline CAS configuration at the component level for MASSs.
b. Four CAS configurations are developed based on different weather and illumination conditions.
c. Risk metrics, critical components, and weak design points pertinent to the failure of the CAS are identified.
d. Risk-reducing measures are recommended, and their effectiveness is evaluated to provide a way forward for risk-informed CAS design.

1.4. Outline

The remaining of this study is organised as follows. Section 2 provides the proposed methodology. Section 3 presents the case study characteristics. Section 4 presents and discusses the derived results. Section 5 summarises the main findings and provides an outlook for future studies.

2. Methodology

The proposed methodology consists of 7 phases, as presented in Fig. 1. In phase 1, the CAS design requirements and assumptions are identified to support the design rationale. In phase 2, IMO instruments pertinent to collision avoidance are reviewed to identify functional and system requirements. In phase 3, a baseline CAS configuration that can adequately satisfy the identified requirements is developed at the component level. In phase 4, risk analysis based on quantitative FTA is conducted in the PTC Windchill (PTC, 2021) environment to derive pertinent risk metrics. In phase 5, criticality analysis of the derived risk metrics is conducted to identify critical components and weak design

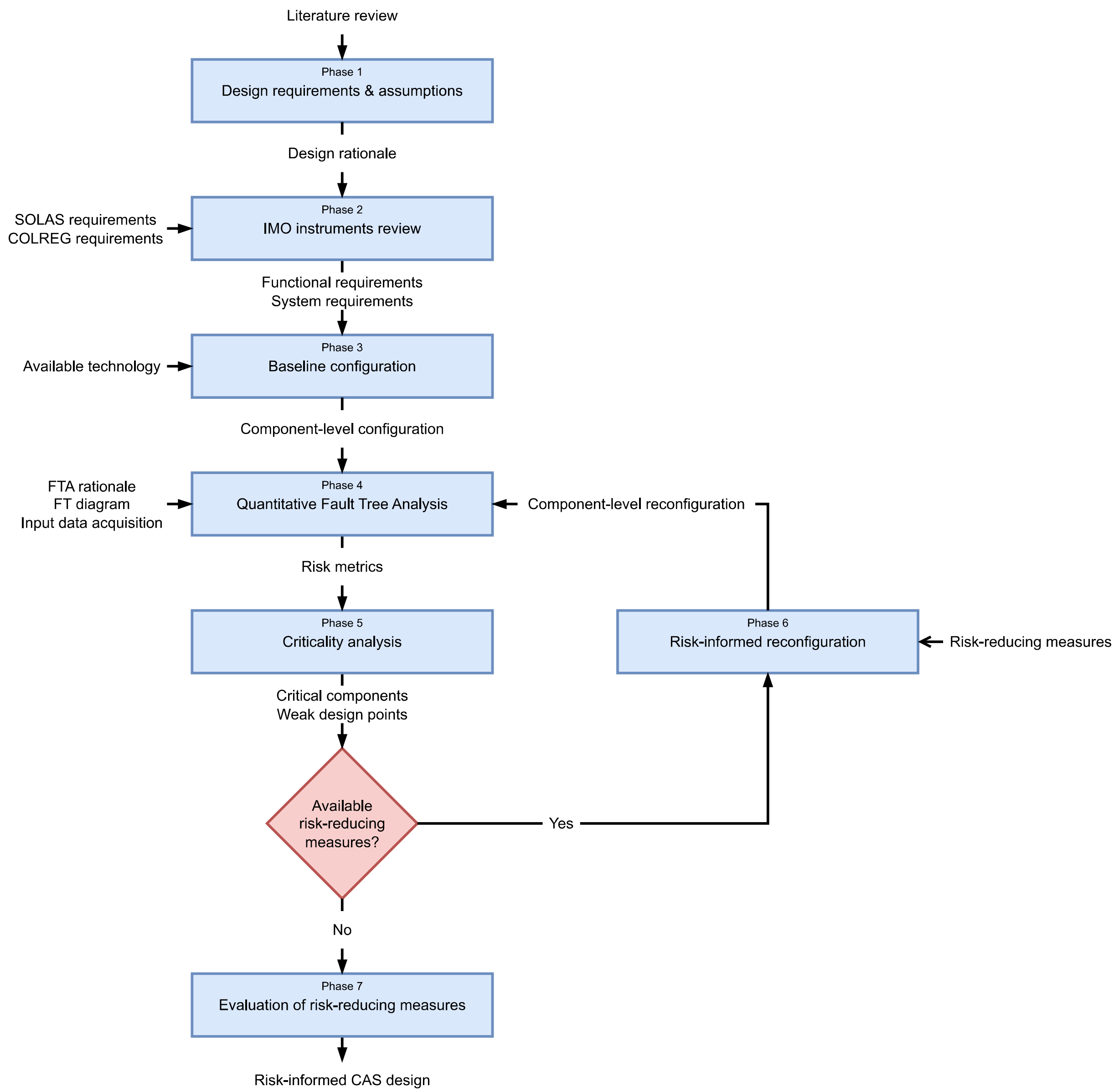

Fig. 1. Flowchart of the proposed methodology.

points. In phase 6, the baseline CAS configuration is reconfigured based on risk-reducing measures to further reduce the identified risk metrics. In phase 7, the effectiveness of the risk-reducing measures is evaluated to support the decision-making of risk-informed CAS design.

Phases 1–5 are further elaborated in the following subsections, whereas the results of phases 4–5 and 6–7 are presented in subsections 4.1-4.3 and 4.4, respectively.

2.1. *Design requirements & assumptions*

In order to conduct risk analysis, a preliminary configuration of the system under-investigation is required at minimum (Dugan et al., 1992). However, one major challenge of new and advanced systems is the lack of information during their early design phase (Rødseth et al., 2021). Thus, the following high-level design requirements are set.

a. The CAS complies to the degree of autonomy four according to IMO (IMO, 2021a) to perform collision avoidance at the same cognitive level as a human operator without any intervention (DNV, 2018; Wu et al., 2020).
b. The CAS complies to the IMO instruments pertinent to collision avoidance to achieve safe collision avoidance amidst the MASSs and conventional ships coexistent maritime scene (Veritas, 2019).

To address these requirements, the following design assumptions are considered.

a. Despite the lack of mandatory instruments dedicated to MASSs, the current IMO instruments can be used as a design reference for the CAS considering small scale amendments, as proposed by the IMO's Maritime Safety Committee during its regulatory scoping exercise (IMO, 2021b).
b. Relevant systems used in conventional ships can be used to approximate the CAS configuration, components list, and even failure data considering the lack of pertinent information for MASSs (Zhang et al., 2022).
c. The lowest level of abstraction for the CAS design is the component level (Rausand, 2014), which is treated as a "black-box" level considering that no further details can be obtained due to the low chance of redesign.

d. The failure of the CAS has catastrophic consequences, which means that it is sufficient to lead to a near-miss collision incident or even collision accident in the autonomous framework (Wróbel et al., 2018a).

2.2. IMO instruments review

In order to comply to the degree of autonomy four according to the IMO (IMO, 2021a), the CAS needs to follow the typical human decision-making process. This process can be translated into its equivalent system functions (Veritas, 2019) that are highly intertwined and interdependent.

a. Information acquisition
b. Information analysis
c. Decision making
d. Action execution

Additionally, in order to comply to the IMO instruments pertinent to collision avoidance, the Convention on the International REGulations for Preventing COLlisions at Sea (COLREG) (IMO, 2018a) and the International Convention for the Safety of Life at Sea (SOLAS)/Chapter V (IMO, 2020) are reviewed. Specifically, the key concepts related to collision avoidance are identified to extrapolate the functional and system requirements for the CAS, as presented in Figs. 2 and 3. For instance, the rule for the ship to proceed at all times at a safe speed (COLREG/Rule 6) is extrapolated as a functional requirement for the CAS to discern the safe speed and as a system requirement to control it in every quarter situation.

Thus, the main systems of the CAS and their functional requirements are as follows

a. Situation Awareness System (SAS) – acquires all the necessary state data of the Own Ship (OS), Target Ships (TSs), and surrounding environment to appraise the quarter situation (COLREG/Rule 5).
b. Decision Making System (DMS) – assesses the collision risk and makes the appropriate collision avoidance decision corresponding to action commands to mitigate the collision risk, determine the safe speed and distance, and exit from the quarter situations (COLREG/Rule 8).
c. Intention Communication System (ICS) – communicates the mutual evasive intentions, emergency, or distress between the OS and TSs of the quarter situation to make the collision avoidance intentions apparent and in timely manner (COLREG/Rule 28).
d. Action Execution System (AES) – activates and controls the necessary actuators to successfully execute the collision avoidance decisions (COLREG/Rule 17).

The main systems can be decomposed into their hierarchically lower subsystems. The subsystems and their functional requirements in forms of their expected input and output are listed in Table 1.

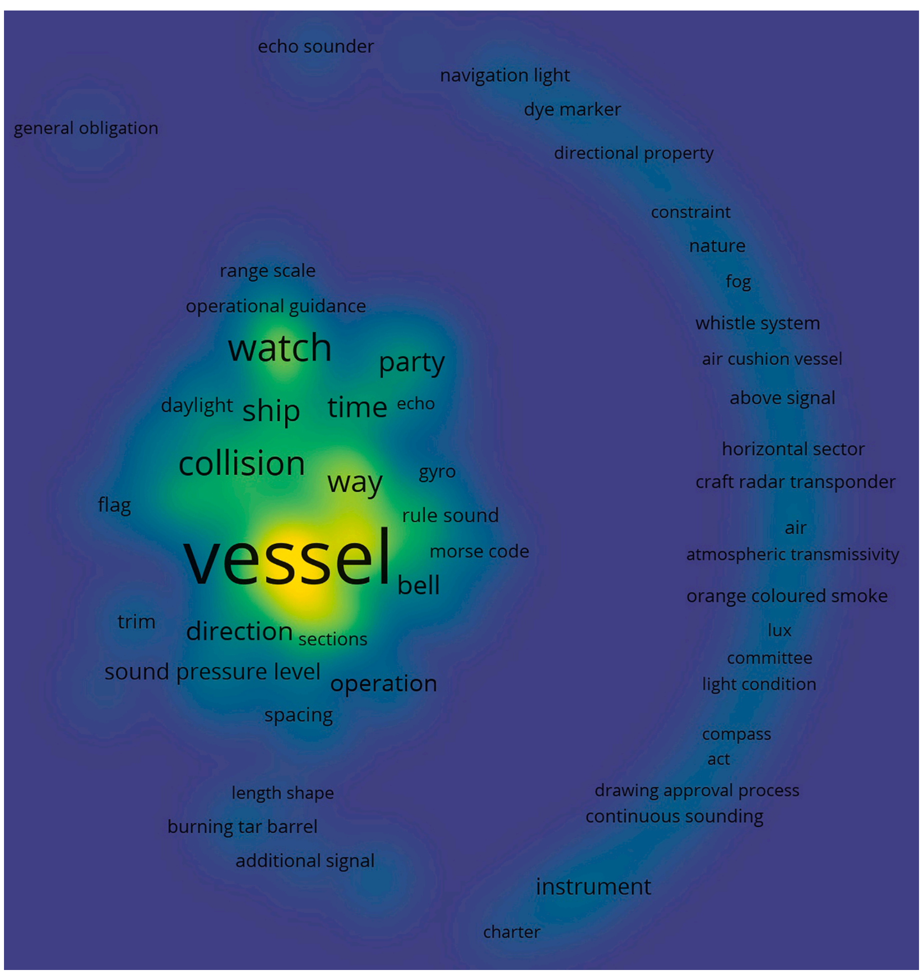

Fig. 2. Density map of the key collision avoidance concepts in the COLREG rules (IMO, 2018a). Bigger font sizes and yellow-coloured clusters indicate greater number of occurrences of key concepts. Density map developed in the VOSviewer (Van Eck and Waltman, 2010) environment.

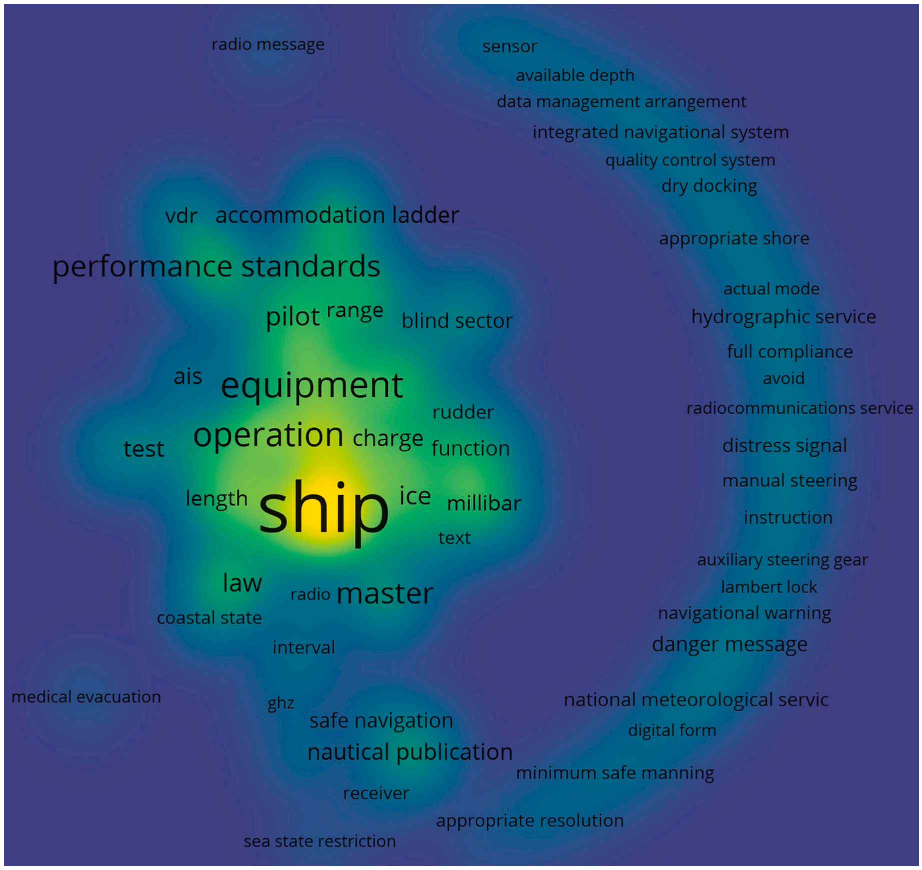

Fig. 3. Density map of the key collision avoidance concepts in the SOLAS/Chapter V (IMO, 2020). Bigger font sizes and yellow-coloured clusters indicate greater number of occurrences of key concepts. Density map developed in the VOSviewer (Van Eck and Waltman, 2010) environment.

Table 1
Subsystems of the CAS and their functional requirements in forms of their expected input and output.

Overall system	Main system	Subsystem	Input	Output	Relevant regulation
Collision Avoidance System (CAS)	Situation Awareness System (SAS)	Medium-Range Scanning System	Light, image, etc.	Obstacle tracking, distance data, etc.	COLREG/Rule 7.c
		Long-Range Scanning System	Radio frequency data, etc.	Distance data, speed data, direction data, etc.	COLREG/Rule 7.b
		Environment Perception System	Temperature data, humidity data, etc.	Weather analysis, weather warnings, etc.	COLREG/Rule 28
		Sound Perception System	Acoustic signals, contextual data, etc.	Sound recognition, sound localisation, etc.	SOLAS/Chapter V/ Regulation 19.2.1.8
		Own-State Perception System	Satellite signals, accelerometer data, gyroscope data, etc.	Position, orientation, velocity, time, etc.	SOLAS/Chapter V/ Regulation 19.2.1.1
		Nautical Chart System	Nautical information, survey data, meteorological data, etc.	Nautical charts, warnings, reports, etc.	SOLAS/Chapter V/ Regulation 27
	Decision Making System (DMS)	Computing System	Location data, warnings, etc.	Action commands, future trajectory, good seamanship, etc.	SOLAS/Chapter V/ Regulation 15.5
	Intention Communication System (ICS)	Light Signalling System	Control signal, etc.	Light, visual information, etc.	COLREG/Rule 22
		Shape Signalling System	Video signal, control signal, etc.	Visual information, etc.	COLREG/Rule 27
		Sound Signalling System	Control signal, etc.	Acoustic signal, etc.	COLREG/Rule 33
		Wireless Communication System	Text data, image data, audio data, etc.	Transmitted data, warnings, etc.	SOLAS/Chapter V/ Regulation 14.4
	Action Execution System (AES)	Power Plant System	Fuel, water, control signal, etc.	Electrical power, thrusting power, heat, etc.	COLREG/Rule 19.b
		Shafting & Steering System	Power, control signal, etc.	Propulsion power, speed control, etc.	SOLAS/Chapter V/ Regulation 25

Table 2
Components list of the baseline CAS configuration and their functional competence.

Subsystem	Component	Function	Relevant regulation
Medium-Range Scanning System	Light Detection And Ranging (LiDAR)	High resolution three dimensional scanning observation, tracking, and identification within the detectable range with depth measurements (Jovanović et al., 2022).	COLREG/Rule 5
	Day/night & thermal camera	High resolution visual observation, tracking, and identification over sea at within the visible field of view even in total darkness and adverse weather, such as fog, rain, or snow (DatCon, 2022).	COLREG/Rule 5
Long-Range Scanning System	Automatic Identification System (AIS)	Automatic ship-to-ship or ship-to-shore communication of the ship's navigational related information, such as the ship's identity, type, position, course, speed, and navigational status, monitoring, and tracking (IMO, 2020).	SOLAS/Chapter V/ Regulation 19.2.4
	RAdio Detection And Ranging (RADAR)	Velocity and distance measurements for the identification, tracking, and positioning of other TSs, obstructions, shorelines, and navigational marks (IMO, 2020).	SOLAS/Chapter V/ Regulation 19.2.3.2
Environment Perception System	Visibility & weather sensor	Visibility and present weather condition measurement, such as fog density, precipitation, haze, smoke, and mist (MicroStep-MIS, 2022a).	SOLAS/Chapter V/ Regulation 5
	Anemometer	Magnitude of wind speed and direction measurement (MicroStep-MIS, 2022b).	SOLAS/Chapter V/ Regulation 5
	Current profiler	Magnitude of underwater currents and direction (Sonardyne, 2022).	COLREG/Rule 6.a.v
	Echo sounder	Bathymetric measurement of the seabed (IMO, 2020).	SOLAS/Chapter V/ Regulation 19.2.3.1
Sound Perception System	Microphone	Sound signals and direction capturing (IMO, 2020).	SOLAS/Chapter V/ Regulation 19.2.1.8
Own-State Perception System	Global Navigation Satellite System (GNSS)	True heading, position, velocity, and rate of turn measurement (IMO, 2020).	SOLAS/Chapter V/ Regulation 19.2.1.6
	Inertial Navigation System (INS)	Heading, attitude, and positional data measurement (Teledynemarine, 2021).	SOLAS/Chapter V/ Regulation 19.2.1.1
Nautical Chart System	Electronic Chart Display and Information System (ECDIS)	Ship's route planning and monitoring based on nautical charts and nautical publications (IMO, 2020).	SOLAS/Chapter V/ Regulation 19.2.1.4
Computing System	Computer hardware	Collision avoidance decision making (IMO, 2020).	SOLAS/Chapter V/ Regulation 15.5
	Artificial Intelligence (AI) software	Collision avoidance decision making (IMO, 2020).	SOLAS/Chapter V/ Regulation 15.5
Light Signalling System	Stern light	Ship's navigational status related information, distress, or collision avoidance intention communication (IMO, 2018a).	COLREG/Rule 22
	Masthead light	Ship's navigational status related information, distress, or collision avoidance intention communication (IMO, 2018a).	COLREG/Rule 22
	Side light	Ship's navigational status related information, distress, or collision avoidance intention communication (IMO, 2018a).	COLREG/Rule 22
	All-round light	Ship's navigational status related information, distress, or collision avoidance intention communication (IMO, 2018a).	COLREG/Rule 22
	Towing light	Ship's navigational status related information, distress,or collision avoidance intention communication (IMO, 2018a).	COLREG/Rule 22
	Flashing light	Ship's navigational status related information, distress, or collision avoidance intention communication (IMO, 2018a).	COLREG/Rule 22
Sound Signalling System	Speaker	Ship's navigational status related information, distress, or collision avoidance intention communication (IMO, 2018a).	COLREG/Rule 33
Shape Signalling System	Liquid Crystal Display (LCD) panel	Ship's navigational status related information, distress or collision avoidance intention communication (IMO, 2018a).	COLREG/Rule 27
Wireless Communication System	Radio system	Ship's navigational status related information, distress, collision avoidance intention, or weather communication (IMO, 2020).	SOLAS/Chapter V/ Regulation 19.2.1.6
	Long Term Evolution (LTE) system	Ship's navigational status related information, distress, or collision avoidance intention communication (IMO, 2018a).	SOLAS/Chapter V/ Regulation 19.2.1.6
Power Plant System	Diesel generator	Electrical power generation (Hansen and Wendt, 2015).	COLREG/Rule 19.b
	Electrical system	Generated electrical power management and distribution to shipboard systems (IMO, 2020).	COLREG/Rule 19.b
	Cooling water system	Heat transfer from machinery using a cooling media, such as sea or fresh water (Brocken, 2016).	COLREG/Rule 19.b
	Fuel system	Piping systems for fuel oil bunkering, storage, transfer, offloading, and treatment (IMO, 2020).	COLREG/Rule 19.b
	Main engine	Mechanical power generation for the ship propulsion (Hansen and Wendt, 2015).	COLREG/Rule 19.b
Shafting & Steering System	Shafting	Mechanical power transfer from the engine to the propeller (Murawski, 2018).	COLREG/Rule 19.b
	Steering gear	Torsional force generation to turn the rudder (IMO, 2020).	SOLAS/Chapter V/ Regulation 25

2.3. Baseline configuration

The derived system and functional requirements are used to develop a baseline CAS configuration at the component level, as presented in Table 2 and Fig. 4. Particularly, the configuration consists of the following components groups.

a. Components that are explicitly mentioned in the IMO instruments, such as the Electronic Chart Display and Information System (ECDIS) (SOLAS/Chapter V/Regulation 19.2.1.4).
b. Components that satisfy the requirements of "*other means*", such as the Inertial Navigation System (INS) that can substitute the standard magnetic compass (SOLAS/Chapter V/Regulations 19.2.1.1, 19.2.2.6) by providing accurate attitude and position information in addition to the heading readings (Teledynemarine, 2021).
c. Components that are not explicitly mentioned in the instruments but reflect the state-of-the-art technology, such as the Light Detection And Ranging (LiDAR) that can provide point clouds of the three dimensional space (Jovanović et al., 2022), thus, further support the full appraisal of the quarter situation (COLREG/Rule 5).

However, it should be mentioned that despite the known limitations of some components for MASSs, such as the conventional Power Plant System (Abaei et al., 2021), they are still included in the baseline CAS configuration considering the current limitation of alternative systems (Eriksen et al., 2021; Wu et al., 2020). Redundancy is introduced for a few components, such as the ECDIS to comply to the requirement of a backup arrangement (SOLAS/Chapter V/Regulations 19.2.1.5, 19.2.2.6). Redundancy is also introduced for the computer hardware and AI software for being the core decision-making components (Abduljabbar et al., 2019). Finally, four day/night & thermal cameras and four Liquid Crystal Display (LCD) panels are arranged to ensure 360 degrees of visual lookout and shape signal communication, respectively.

2.4. Quantitative Fault Tree Analysis

2.4.1. Fault Tree analysis rationale

FTA uses graphical symbols and Boolean logic to model the occurrence of a hazardous event in a deductive manner (Bäckström et al., 2016; Sharma and Singh, 2015). FTA is used to identify critical events and weak design points leading to the occurrence of the hazardous event and recommend risk-reducing measures related to system components, structure, and barriers (Rausand and Haugen, 2020). FTA facilitates both qualitative and quantitative risk analysis of complex systems with intertwined hardware and software interactions, as well as new systems where design information is incomplete (IEC, 2006). Thus, its application spans across the analysis of various safety-critical systems, such as nuclear power plants (Purba, 2014), missiles (Yuan and Long, 2010), spacecrafts (Gao et al., 2021), commercial aircraft systems (Changcong et al., 2021), automobiles (James et al., 2018), cyber-security systems (Bolbot et al., 2020), and collision risk alarm systems (Wu et al., 2020).

Since FTA was originally developed to analyse binary static systems, it has several limitations (Hokstad et al., 2012), such as the inability to capture time related dependencies (Ruijters and Stoelinga, 2015), tackle unforeseeable events, and analyse dynamic systems of non-binary state and of complicated maintenance (Rausand and Haugen, 2020). To compensate some of these weaknesses, various FTA extensions have been developed such as dynamic FTs (Dugan et al., 1990), repairable FTs (Bobbio and Raiteri, 2004), and fuzzy FTs (Tanaka et al., 1983). However, since the developed baseline CAS configuration of this study considers a straight-forward decomposition into its components, the use of a static FT is considered to be adequate.

2.4.2. Fault Tree diagram

To conduct FTA, a hazardous event, referred as the Top Event (TE) (IEC, 2006), must be defined and systematically developed into a FT diagram (Misra, 2008). The FT diagram is developed by analysing the TE into its subsequent causal events, known as the Intermediate Events (IEs), using logical gates that reflect their causal relationship (Muhammad et al., 2010). In this study, the failure of the CAS is defined as the TE, which is decomposed into the failure of its main systems using an "OR" gate. This indicates that the failure of at least one of the main systems is sufficient to lead to the failure of the whole system.

The FT diagram is further developed by analysing the IEs into their subsequent causal events, known as the Basic Events (BEs), that represent simpler forms of failures (Bäckström et al., 2016). In this study, the BEs represent the failure of the components. It should be mentioned that regarding the Power Plant System and Shafting & Steering System, risk-reducing measures have already been conducted in (Brocken, 2016) within the MASS framework. For this reason, these systems are not further analysed into their components but considered as a single propulsion & steering component. "OR" gates are used for components with no functional diversity (Rausand and Hoyland, 2003), such as the visibility & weather sensor, anemometer, current profiler, and echo sounder. "AND" gates are used for components with functional diversity, such as the INS and Global Navigation Satellite System (GNSS). "VOTE" gates are used for redundant components, such as the ECDIS. A graphical representation of the developed FT diagram and description of each event are presented in Fig. 5 and Table 3, respectively.

2.4.3. Input data acquisition

To quantitatively analyse a FT diagram and derive pertinent risk metrics, the BEs need to be embedded with appropriate input data, such as the probability of failure, failure rate, or Mean Time Between Failure (MTBF) (Ugurlu and Cicek, 2022). MTBF is a basic reliability measure of stochastic nature that is equal to the inverse of the failure rate and denotes the mean time between two successive failures (Kumar et al., 1999) usually presented in units of hours. The use of MTBF data enables the modelling of continuous-time FTs that considers the evolution of a system failure over time (Ruijters and Stoelinga, 2015). It enables the investigation of the accident event rather than the total downtime after the accident (Torell and Avelar, 2004), which is the primary focus of safety-critical autonomous systems. Finally, it enables the risk analysis of new systems when time, practicality, scarcity of data, and pace of technology development are of their most barriers (Krasich, 2009).

The MTBF data acquisition is based on the following assumptions.

a. MTBF of each component is statistically independent (Ruijters and Stoelinga, 2015).
b. MTBF is independent of external influences of the operating conditions, such as variations of humidity, temperature, and stress levels (Krasich, 2009).
c. MTBF considers constant failure rate in the normal operating period of the "bathtub curve" (Torell and Avelar, 2004).
d. MTBF is restored after repair (Xiao et al., 2007) but the components are non-repairable during the operation (Dugan et al., 1992).

The acquired MTBF data based on the available literature and reported data are presented in Table 4. It is worth mentioning that considering all the uncertainties pertaining to the actual system, emphasis shall be given on the order of magnitude and not on the exact values of the acquired data (Cheok et al., 1998). Finally, the MTBF is acquired even for the non-repairable components, such as the navigational lights, which is a commonly accepted practice (Krasich, 2009; PTC, 2021).

2.5. Criticality analysis

Criticality analysis is conducted to identify critical BEs and failure mechanisms (Singh et al., 2022). In this study, the probability of failures of the events are used to identify the major contributors to the occurrence of the TE (IEC, 2006). Additionally, the Birnbaum (I^B), Criticality (I^{CR}), and Fussell-Vesely (I^{FV}) Importance measures are used to rank the importance of the BEs (Rausand and Hoyland, 2003). Specifically, the I^B calculates the probability that the BE is critical to the occurrence of the TE (Xing and Amari, 2008); the I^{CR} calculates the conditional probability that the BE is critical and occurred given that the TE has occurred (Aven, 1985); and, the I^{FV} calculates the conditional probability that at least one Minimal Cut Set (MCS) containing the BE is failed given that the TE has occurred (Rausand and Haugen, 2020), giving similar results to the I^{CR}. Finally, the probability of failures of the MCSs are used to rank the importance of the failure mechanisms (Ruijters and Stoelinga, 2015), where MCS stands for a cut set with the minimum number of BEs that when occurred simultaneously leads to the occurrence of the TE (Rausand, 2014).

3. Case study

The proposed methodology is applied in a case study that considers a SSS cargo ship operation. Limiting the operating scenario to SSS, which is defined as a coastal trading with routes up to 800 nautical miles (Ametller, 2015; Bjornland, 1993), is deemed to be a pivotal step to analyse the risk associated with the CAS before the full-scale

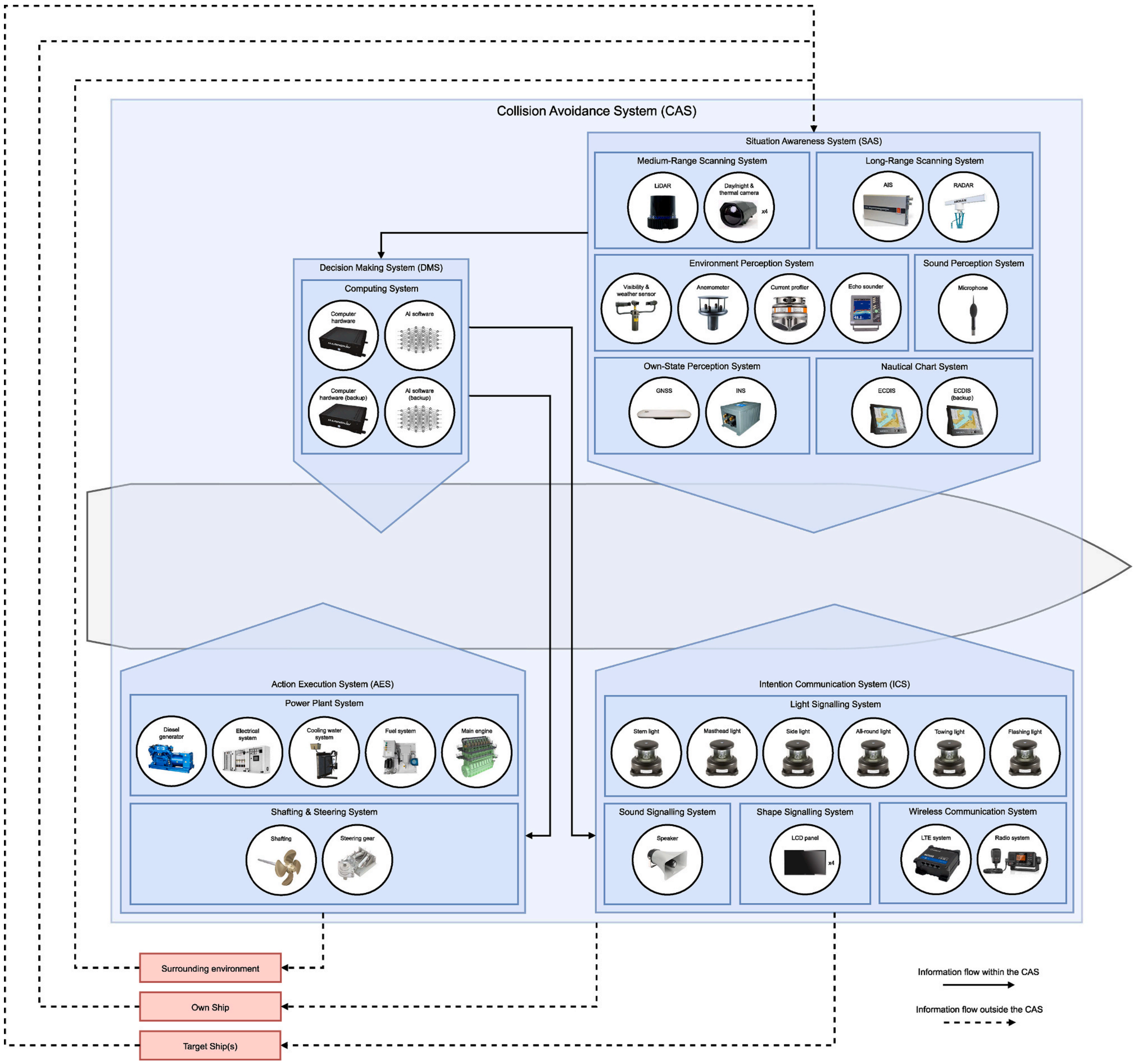

Fig. 4. Schematic representation of the developed baseline CAS configuration at the component level. Arrows indicate the direction of information flow.

implementation for transoceanic operations. The main particulars of the investigated ship are presented in Table 5.

The investigated ship is considered to operate autonomously only during the en route phase for a total of 730 h (Zhang et al., 2022), which is equivalent to one month of operation prior to maintenance. Yet, the en route phase for cargo ships constitutes the most unsafe phase that contributes up to 40% of the total accident occurrences (EMSA, 2021). Particularly, a typical SSS route at the North Sea can lead to quarter situation of up to 10 TSs within a 5 nautical miles range and traffic separation lines with density of up to 200,000 routes per 0.08 km per year, as shown in Fig. 6.

Four different operating modes are investigated based on the combinations of weather and illumination conditions, as presented in Table 6. Specifically, good weather considers calm sea and good visibility, whereas adverse weather considers heavy sea state with restricted visibility. Currents are considered to exist in all weather conditions. Daylight and darkness illuminations consider 12 h from sunrise to sunset and 12 h from sunset to sunrise, respectively.

The case study specific customisations needed for the baseline CAS configuration are the requirements for two masthead lights (COLREG/Rules 23.a.i-ii), two side lights for the starboard and port sides (COLREG/Rule 21.b), and five all-round lights (COLREG/Rules 28, 34.b.iii, 34.d, 36). The mode specific customisations are listed in Table 7.

4. Results & discussion

4.1. Probability of failure

The probability of failures derived from the FTA are presented in Table 8 and Figure B.1-Figure B.11. The results indicate that the lowest probability of failure exhibits the CAS in mode 1 being as low as 11% when operated for 730 h. The CAS in mode 3 exhibits the highest probability of failure reaching up to 32%. The percentage contributions of each IE to the TE indicate that the ICS is the most critical main system, followed by the SAS. Specifically, the probability of failure of the ICS reaches from 4% in mode 1 as high as 25% in mode 3.

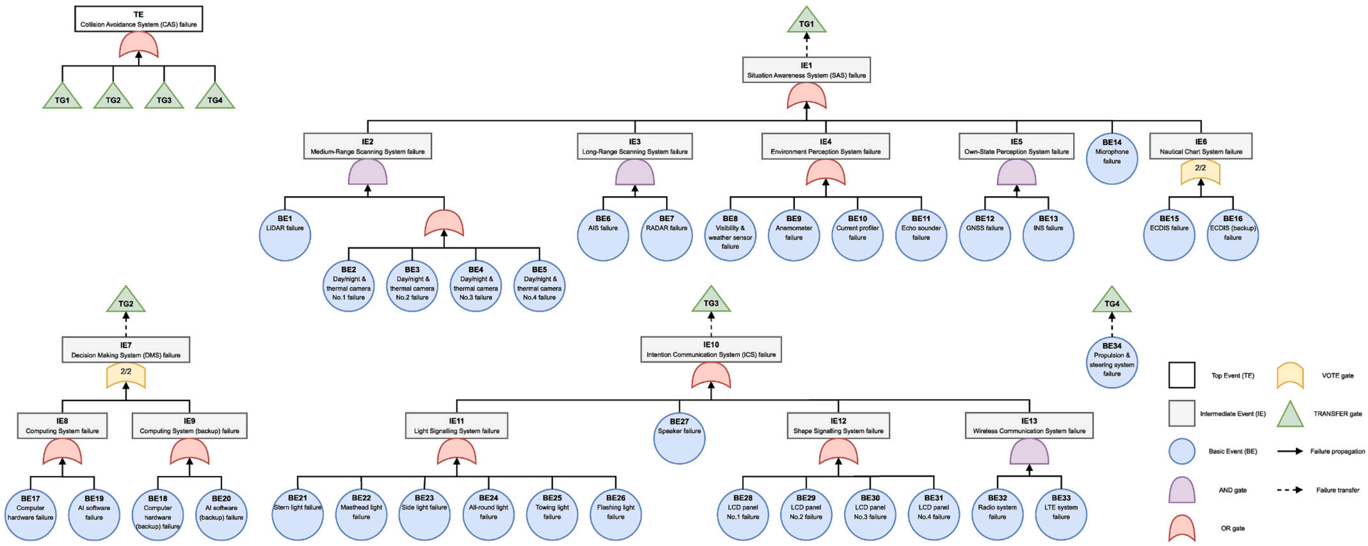

Fig. 5. Graphical representation of the baseline CAS configuration developed into a FT diagram.

Table 3
Description of the events in the developed FT diagram.

Event	Description	Event	Description
TE	Collision Avoidance System (CAS) failure	BE11	Echo sounder failure
IE1	Situation Awareness System (SAS) failure	BE12	GNSS failure
IE2	Medium-Range Scanning System failure	BE13	INS failure
IE3	Long-Range Scanning System failure	BE14	Microphone failure
IE4	Environment Perception System failure	BE15	ECDIS failure
IE5	Own-State Perception System failure	BE16	ECDIS (backup) failure
IE6	Nautical Chart System failure	BE17	Computer hardware failure
IE7	Decision Making System (DMS) failure	BE18	Computer hardware (backup) failure
IE8	Computing System failure	BE19	AI software failure
IE9	Computing System (backup) failure	BE20	AI software (backup) failure
IE10	Intention Communication System (ICS) failure	BE21	Stern light failure
IE11	Light Signalling System failure	BE22	Masthead light failure
IE12	Shape Signalling System failure	BE23	Side light failure
IE13	Wireless Communication System failure	BE24	All-round light failure
BE1	LiDAR failure	BE25	Towing light failure
BE2	Day/night & thermal camera No.1 failure	BE26	Flashing light failure
BE3	Day/night & thermal camera No.2 failure	BE27	Speaker failure
BE4	Day/night & thermal camera No.3 failure	BE28	LCD panel No.1 failure
BE5	Day/night & thermal camera No.4 failure	BE29	LCD panel No.2 failure
BE6	AIS failure	BE30	LCD panel No.3 failure
BE7	RADAR failure	BE31	LCD panel No.4 failure
BE8	Visibility & weather sensor failure	BE32	Radio system failure
BE9	Anemometer failure	BE33	LTE system failure
BE10	Current profiler failure	BE34	Propulsion & steering system

Table 4
Acquired MTBF data for each BE.

BE	Component	MTBF in 10^3 h	Reference
BE1	Quanergy Systems “M1 Edge”	60	(Quanergy, 2022)
BE2-5	DAT – CON “CLRT/HD-400”	20.2	(DatCon, 2022)
BE6	Kongsberg Maritime “AIS 300S”	100	(Kongsberg, 2020)
BE7	Micra “REKA”	87.6	(Micran, 2022)
BE8	MicroStep-MIS “VPF-730”’	56.7	(MicroStep-MIS, 2022a)
BE9	MicroStep-MIS “Windsonic 75 Anemometer”	131.4	(MicroStep-MIS, 2022b)
BE10	Sonardyne “Syrinx”	225	(Sonardyne, 2022)
BE11	Nautel Sonar “NESDF”	20	(NautelSonar, 2020)
BE12	Kongsberg Maritime “SEANAV 300 Series”	45	(Kongsberg, 2018)
BE13	Teledyne Marine “MK31”	16	(Teledynemarine, 2021)
BE14	BKSV “UA-1404”	40	(BrüelKjær, 2009)
BE15-16	Moxa “MPC-122-K Series”	39.675	(DigitX, 2020)
BE17-18	MarineNav “LEVIATHAN 17i FANLESS”	100	(MarineNav, 2020)
BE19-20	–	40	(Xu et al., 2013)
BE21-26	Oxley “Series 1” & “Series 2”	30	(Oxleygroup, 2022)
BE27	Zenitel “VML-1520”	1,500	(Zenitel, 2022)
BE28-30	Litemax “DLF/DLH1968-U”	70	(Litemax, 2021)
BE31	Danphone “DCB 9140 IP”	50	(Danphone, 2022)
BE32	Teltonika Networks “RUT950”	270	(Teltonika, 2019)
BE33	–	42.048	(Brocken, 2016)

4.2. Importance measures

The derived Importance measures are provided in Table 9. The first notable observation is that the ranking concerning the order of magnitude is consistent across all Importance measures and modes, expect for the speaker and LTE system. Considering that the two factors affecting the Importance measures are the location of the BEs in the FT diagram and their input data (Rausand, 2014), this consistency suggests the embedment of reasonable MTBF data and the robustness of the developed FT diagram to represent the failure of the CAS. This is particularly pivotal for this early design phase considering the great uncertainties pertaining to the actual CAS design that is currently unknown. This also suggests that no sensitivity analysis is required at this design phase.

In addition, the robustness of the FT diagram enables the identification of the most critical components that exhibit the highest Importance measures. The results indicate that the BEs with the highest Importance measures are the echo sounder, navigational lights, microphone, visibility & weather sensor, propulsion & steering system, LCD panels, anemometer, current profiler, and speaker. It can be deduced

Table 5
Main particulars of the investigated ship.

Particular	Value
Length overall	75.0 m
Length between perpendiculars	73.0 m
Breadth	13.5 m
Draught	5.0 m
Gross tonnage	2150 tonnes
Deadweight	1750 tonnes
Operating speed	12.4 knots

that 67% of them are components of the ICS, followed by 28% of the SAS.

4.3. Minimal Cut Sets

The MCS results are presented in Table 10. First, it can be noted that the MCSs are of order 1 or 2. MCSs with lower order are more critical (Rausand, 2014), since a cut set with fewer BEs is more likely be in a failure state (Ruijters and Stoelinga, 2015). In addition, a BE contained in many different MCSs is critical as it contributes more towards the failure of the whole system (Xu et al., 2013).

The components that exhibit the most vulnerable failure mechanisms are the echo sounder, followed by the navigational lights, microphone, propulsion & steering system, visibility & weather sensor, LCD panels, anemometer, current profiler, AI software and its backup, and computer hardware and its backup. It is worth mentioning that 48% of all MCSs are components of the ICS, followed by 36% of the SAS.

Finally, the effectiveness of redundancy in reducing the pertinent risk metrics can be noted, whether in forms of identical components or functional diversity. For instance, despite INS and echo sounder exhibiting the lowest MTBF, adding functional diversity to the INS through the GNSS leads to a reduction of its criticality of up to two orders of magnitude both as a component and failure mechanism compared to the echo sounder.

4.4. Risk-informed reconfiguration & evaluation of risk-reducing measures

For brevity, risk-informed reconfiguration is conducted only for the CAS in mode 3 that exhibits the highest probability of failure. A typical cost-effective risk-reducing measure is to focus on the critical components and failure mechanisms by either using alternative components with better reliability or introducing redundancy (Rausand and Haugen, 2020). However, considering that alternative components for MASSs are yet to be developed, redundancy is added to the relatively inexpensive but critical components of the ICS and SAS. These are the echo sounder, current profiler, visibility & weather sensor, anemometer, microphone, LCD panels, navigational lights, and speaker.

The FTA results of the risk-informed CAS reconfiguration are presented in Table 11-13 and Figure B.12-Figure B.14. The derived results indicate 3% probability of failure of the risk-informed CAS reconfiguration when operated for 730 h, which equals to a reduction of 91% compared to the previous baseline CAS configuration. This is attributes to the reductions of the probability of failures of the ICS from 25% to 0.6% and SAS from 8% to 0.5%. Particularly, the Importance measures of the critical components and probability of failures of the MCSs are reduced up to three and four orders of magnitude, respectively. Additionally, it is noted that the ranking of the order of magnitude of the Importance measures continuous to be consistent, except for the LTE system. Both the reduction of the probability of failure of the risk-informed CAS reconfiguration and the consistency in the ranking of the Importance measures verify the robustness of the developed FT diagram that magnifies the effectiveness of risk-reducing measures when

Table 6
Four operating modes based on different weather and illumination conditions.

	Daylight illumination	Darkness illumination
Good weather	Mode 1	Mode 2
Adverse weather	Mode 3	Mode 4

Table 7
Customisation of the baseline CAS configuration based on each mode.

Component	Mode 1	Mode 2	Mode 3	Mode 4	Relevant regulation
LCD panels	✓	×	✓	×	COLREG/Rule 20.d
Navigational lights	×	✓	✓	✓	COLREG/Rules 20.b-c
Towing light	×	×	×	×	COLREG/Rule 24
Flashing light	×	×	×	×	COLREG/Rule 23
Anemometer	×	×	✓	✓	COLREG/Rule 6
Visibility & weather sensor	×	×	✓	✓	COLREG/Rule 6

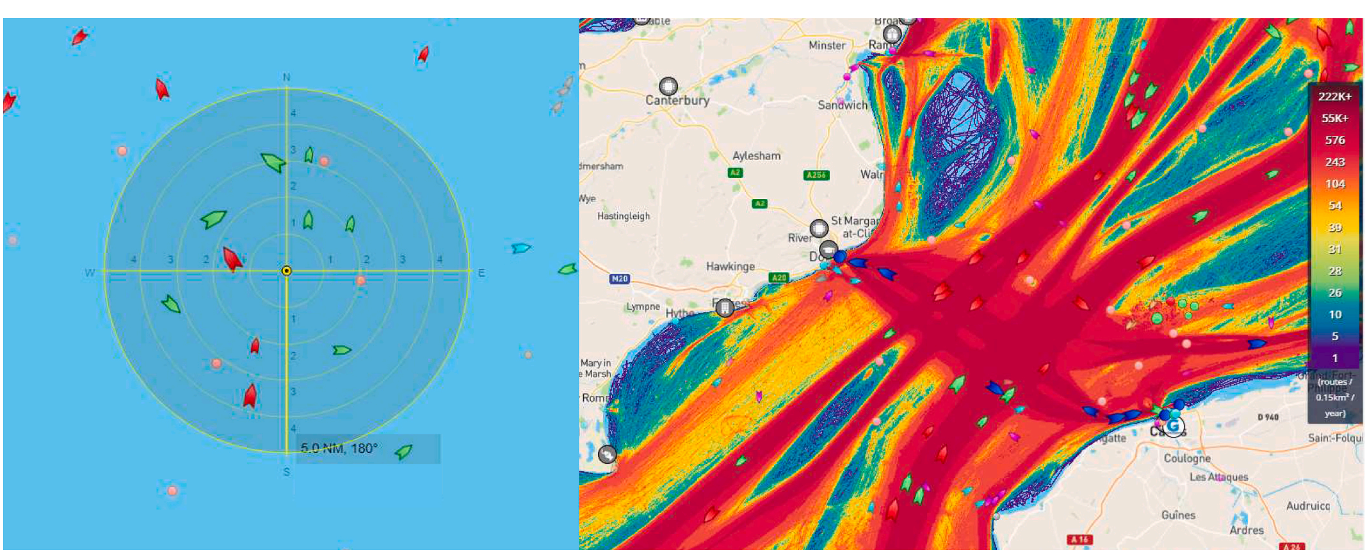

Fig. 6. Number of TSs within a 5 nautical miles range and traffic density considering a SSS route at the Strait of Dover. AIS data derived from marinetraffic.com.

Table 8
Probability of failures of the TE and IEs and the percentage contributions of each IE to the TE in each mode.

Event		Probability of failure at 730 h							
		Mode 1		Mode 2		Mode 3		Mode 4	
TE	CAS failure	$1.14\ 10^{-1}$		$2.76\ 10^{-1}$		$3.18\ 10^{-1}$		$2.89\ 10^{-1}$	
IE	SAS failure	$5.89\ 10^{-2}$	51.72%	$5.89\ 10^{-2}$	21.37%	$7.61\ 10^{-2}$	23.93%	$7.61\ 10^{-2}$	26.34%
	DMS failure	$6.36\ 10^{-4}$	0.56%	$6.36\ 10^{-4}$	0.23%	$6.36\ 10^{-4}$	0.20%	$6.36\ 10^{-4}$	0.22%
	ICS failure	$4.14\ 10^{-2}$	36.30%	$2.16\ 10^{-1}$	78.48%	$2.48\ 10^{-1}$	78.12%	$2.16\ 10^{-1}$	74.89%
	AES failure	$1.72\ 10^{-2}$	15.11%	$1.72\ 10^{-2}$	6.24%	$1.72\ 10^{-2}$	5.41%	$1.72\ 10^{-2}$	5.96%

Table 9
Importance measures of the BEs in each mode.

BE	Mode 1		Mode 2		Mode 3		Mode 4	
	I^B	I^{FV} or I^{CR}	I^B	I^{FV} or I^{CR}	I^B	I^{FV} or I^{CR}	I^B	I^{FV} or I^{CR}
Echo sounder	1.00	$2.99\ 10^{-1}$	1.00	$1.12\ 10^{-1}$	1.00	$9.47\ 10^{-2}$	1.00	$1.06\ 10^{-1}$
Stern light	–	–	1.00	$7.54\ 10^{-2}$	1.00	$6.35\ 10^{-2}$	1.00	$7.13\ 10^{-2}$
Masthead light No.1	–	–	1.00	$7.54\ 10^{-2}$	1.00	$6.35\ 10^{-2}$	1.00	$7.13\ 10^{-2}$
Masthead light No.2	–	–	1.00	$7.54\ 10^{-2}$	1.00	$6.35\ 10^{-2}$	1.00	$7.13\ 10^{-2}$
Starboard-side light	–	–	1.00	$7.54\ 10^{-2}$	1.00	$6.35\ 10^{-2}$	1.00	$7.13\ 10^{-2}$
Port-side light	–	–	1.00	$7.54\ 10^{-2}$	1.00	$6.35\ 10^{-2}$	1.00	$7.13\ 10^{-2}$
All-round light No.1	–	–	1.00	$7.54\ 10^{-2}$	1.00	$6.35\ 10^{-2}$	1.00	$7.13\ 10^{-2}$
All-round light No.2	–	–	1.00	$7.54\ 10^{-2}$	1.00	$6.35\ 10^{-2}$	1.00	$7.13\ 10^{-2}$
All-round light No.3	–	–	1.00	$7.54\ 10^{-2}$	1.00	$6.35\ 10^{-2}$	1.00	$7.13\ 10^{-2}$
All-round light No.4	–	–	1.00	$7.54\ 10^{-2}$	1.00	$6.35\ 10^{-2}$	1.00	$7.13\ 10^{-2}$
All-round light No.5	–	–	1.00	$7.54\ 10^{-2}$	1.00	$6.35\ 10^{-2}$	1.00	$7.13\ 10^{-2}$
Microphone	1.00	$1.51\ 10^{-1}$	1.00	$5.67\ 10^{-2}$	1.00	$4.78\ 10^{-2}$	1.00	$5.36\ 10^{-2}$
Propulsion & steering system	1.00	$1.44\ 10^{-1}$	1.00	$5.40\ 10^{-2}$	1.00	$4.55\ 10^{-2}$	1.00	$5.11\ 10^{-2}$
Visibility & weather sensor	–	–	–	–	1.00	$3.38\ 10^{-2}$	1.00	$3.79\ 10^{-2}$
LCD panel No.1	1.00	$8.65\ 10^{-2}$	–	–	1.00	$2.74\ 10^{-2}$	–	–
LCD panel No.2	1.00	$8.65\ 10^{-2}$	–	–	1.00	$2.74\ 10^{-2}$	–	–
LCD panel No.3	1.00	$8.65\ 10^{-2}$	–	–	1.00	$2.74\ 10^{-2}$	–	–
LCD panel No.4	1.00	$8.65\ 10^{-2}$	–	–	1.00	$2.74\ 10^{-2}$	–	–
Anemometer	–	–	–	–	1.00	$1.46\ 10^{-2}$	1.00	$1.64\ 10^{-2}$
Current profiler	1.00	$2.70\ 10^{-2}$	1.00	$1.02\ 10^{-2}$	1.00	$8.56\ 10^{-3}$	1.00	$9.61\ 10^{-3}$
LiDAR	$1.42\ 10^{-1}$	$1.43\ 10^{-2}$	$1.42\ 10^{-1}$	$5.39\ 10^{-3}$	$1.42\ 10^{-1}$	$4.53\ 10^{-3}$	$1.42\ 10^{-1}$	$5.09\ 10^{-3}$
GNSS	$4.46\ 10^{-2}$	$5.99\ 10^{-3}$	$4.46\ 10^{-2}$	$2.25\ 10^{-3}$	$4.46\ 10^{-2}$	$1.90\ 10^{-3}$	$4.46\ 10^{-2}$	$2.13\ 10^{-3}$
INS	$1.61\ 10^{-2}$	$5.99\ 10^{-3}$	$1.61\ 10^{-2}$	$2.25\ 10^{-3}$	$1.61\ 10^{-2}$	$1.90\ 10^{-3}$	$1.61\ 10^{-2}$	$2.13\ 10^{-3}$
Speaker	1.00	$4.06\ 10^{-3}$	1.00	$1.53\ 10^{-3}$	1.00	$1.29\ 10^{-3}$	1.00	$1.44\ 10^{-3}$
AI software	$2.54\ 10^{-2}$	$3.83\ 10^{-3}$	$2.54\ 10^{-2}$	$1.44\ 10^{-3}$	$2.54\ 10^{-2}$	$1.21\ 10^{-3}$	$2.54\ 10^{-2}$	$1.36\ 10^{-3}$
AI software (backup)	$2.54\ 10^{-2}$	$3.83\ 10^{-3}$	$2.54\ 10^{-2}$	$1.44\ 10^{-3}$	$2.54\ 10^{-2}$	$1.21\ 10^{-3}$	$2.54\ 10^{-2}$	$1.36\ 10^{-3}$
Day/night & thermal camera No.1	$1.21\ 10^{-2}$	$3.58\ 10^{-3}$	$1.21\ 10^{-2}$	$1.35\ 10^{-3}$	$1.21\ 10^{-2}$	$1.13\ 10^{-3}$	$1.21\ 10^{-2}$	$1.27\ 10^{-3}$
Day/night & thermal camera No.2	$1.21\ 10^{-2}$	$3.58\ 10^{-3}$	$1.21\ 10^{-2}$	$1.35\ 10^{-3}$	$1.21\ 10^{-2}$	$1.13\ 10^{-3}$	$1.21\ 10^{-2}$	$1.27\ 10^{-3}$
Day/night & thermal camera No.3	$1.21\ 10^{-2}$	$3.58\ 10^{-3}$	$1.21\ 10^{-2}$	$1.35\ 10^{-3}$	$1.21\ 10^{-2}$	$1.13\ 10^{-3}$	$1.21\ 10^{-2}$	$1.27\ 10^{-3}$
Day/night & thermal camera No.4	$1.21\ 10^{-2}$	$3.58\ 10^{-3}$	$1.21\ 10^{-2}$	$1.35\ 10^{-3}$	$1.21\ 10^{-2}$	$1.13\ 10^{-3}$	$1.21\ 10^{-2}$	$1.27\ 10^{-3}$
ECDIS	$1.82\ 10^{-2}$	$2.77\ 10^{-3}$	$1.82\ 10^{-2}$	$1.04\ 10^{-3}$	$1.82\ 10^{-2}$	$8.78\ 10^{-4}$	$1.82\ 10^{-2}$	$9.86\ 10^{-4}$
ECDIS (backup)	$1.82\ 10^{-2}$	$2.77\ 10^{-3}$	$1.82\ 10^{-2}$	$1.04\ 10^{-3}$	$1.82\ 10^{-2}$	$8.78\ 10^{-4}$	$1.82\ 10^{-2}$	$9.86\ 10^{-4}$
Computer hardware	$2.54\ 10^{-2}$	$1.54\ 10^{-3}$	$2.54\ 10^{-2}$	$5.79\ 10^{-4}$	$2.54\ 10^{-2}$	$4.87\ 10^{-4}$	$2.54\ 10^{-2}$	$5.47\ 10^{-4}$
Computer hardware (backup)	$2.54\ 10^{-2}$	$1.54\ 10^{-3}$	$2.54\ 10^{-2}$	$5.79\ 10^{-4}$	$2.54\ 10^{-2}$	$4.87\ 10^{-4}$	$2.54\ 10^{-2}$	$5.47\ 10^{-4}$
AIS	$8.30\ 10^{-3}$	$5.04\ 10^{-4}$	$8.30\ 10^{-3}$	$1.89\ 10^{-4}$	$8.30\ 10^{-3}$	$1.59\ 10^{-4}$	$8.30\ 10^{-3}$	$1.79\ 10^{-4}$
RADAR	$7.27\ 10^{-3}$	$5.04\ 10^{-4}$	$7.27\ 10^{-3}$	$1.89\ 10^{-4}$	$7.27\ 10^{-3}$	$1.59\ 10^{-4}$	$7.27\ 10^{-3}$	$1.79\ 10^{-4}$
LTE system	$1.45\ 10^{-2}$	$3.27\ 10^{-4}$	$1.45\ 10^{-2}$	$1.23\ 10^{-4}$	$1.45\ 10^{-2}$	$1.03\ 10^{-4}$	$1.45\ 10^{-2}$	$1.16\ 10^{-4}$
Radio system	$2.70\ 10^{-3}$	$3.27\ 10^{-4}$	$2.70\ 10^{-3}$	$1.23\ 10^{-4}$	$2.70\ 10^{-3}$	$1.03\ 10^{-4}$	$2.70\ 10^{-3}$	$1.16\ 10^{-4}$

proper decision-making concerning the most critical components and failure mechanisms are taken in the right direction.

The derived results are compared against the values reported in the pertinent literature. (Zhang et al., 2022) reported 5.5% probability of contact accidents for a remotely controlled ship during the operation of 720 h, which was attributed to probability of failures of 1.7%, 3.7%, 0.2%, corresponding to the AES, SAS, and DMS, respectively. For conventional ships (Goerlandt and Kujala, 2011), concluded that 0.26 collision accidents are estimated per year, which is equivalent to 2.17% probability of collisions per month. In both cases, the results range at the same order of magnitude as found in this study. However, it should be underlined that the failure of the CAS does not necessarily lead to a collision accident, thus, the comparison of the results is facilitated only for verification purposes.

It is worth noting that in this risk-informed CAS reconfiguration, the AES is the major contributor to the failure of the overall system. This is aligned with the notion that mechanical components of MASSs, especially the Power Plant System, will have much higher failure rates compared to other systems (Eriksen et al., 2021; Kretschmann et al., 2015). However, this observation adds another layer of interest as the propulsion & steering component already represents a risk-informed configuration as mentioned earlier with a backup main engine. This indicates the limitation of redundancy as an effective risk-reducing measure for the Power Plant System and the need for intelligent

Table 10
Probability of failures of the MCSs in each mode.

MCS	Probability of failure			
	Mode 1	Mode 2	Mode 3	Mode 4
{Echo sounder}	2.99 10^{-1}	1.12 10^{-1}	9.47 10^{-2}	1.06 10^{-1}
{Masthead light No.1}	–	7.54 10^{-2}	6.35 10^{-2}	7.13 10^{-2}
{Masthead light No.2}	–	7.54 10^{-2}	6.35 10^{-2}	7.13 10^{-2}
{Starboard-side light}	–	7.54 10^{-2}	6.35 10^{-2}	7.13 10^{-2}
{Port-side light}	–	7.54 10^{-2}	6.35 10^{-2}	7.13 10^{-2}
{All-round light No.1}	–	7.54 10^{-2}	6.35 10^{-2}	7.13 10^{-2}
{All-round light No.2}	–	7.54 10^{-2}	6.35 10^{-2}	7.13 10^{-2}
{All-round light No.3}	–	7.54 10^{-2}	6.35 10^{-2}	7.13 10^{-2}
{All-round light No.4}	–	7.54 10^{-2}	6.35 10^{-2}	7.13 10^{-2}
{All-round light No.5}	–	7.54 10^{-2}	6.35 10^{-2}	7.13 10^{-2}
{Stern light}	–	7.54 10^{-2}	6.35 10^{-2}	7.13 10^{-2}
{Microphone}	1.51 10^{-1}	5.67 10^{-2}	4.78 10^{-2}	5.36 10^{-2}
{Propulsion & steering system}	1.44 10^{-1}	5.40 10^{-2}	4.55 10^{-2}	5.11 10^{-2}
{Visibility & weather sensor}	–	–	3.38 10^{-2}	3.79 10^{-2}
{LCD panel No.1}	8.65 10^{-2}	–	2.74 10^{-2}	–
{LCD panel No.2}	8.65 10^{-2}	–	2.74 10^{-2}	–
{LCD panel No.3}	8.65 10^{-2}	–	2.74 10^{-2}	–
{LCD panel No.4}	8.65 10^{-2}	–	2.74 10^{-2}	–
{Anemometer}	–	–	1.46 10^{-2}	1.64 10^{-2}
{Current profiler}	2.70 10^{-2}	1.02 10^{-2}	8.56 10^{-3}	9.61 10^{-3}
{INS, GNSS}	5.99 10^{-3}	2.25 10^{-3}	1.90 10^{-3}	2.13 10^{-3}
{Speaker}	4.06 10^{-3}	1.53 10^{-3}	1.29 10^{-3}	1.44 10^{-3}
{Day/night & thermal camera No.1, LiDAR}	3.58 10^{-3}	1.35 10^{-3}	1.13 10^{-3}	1.27 10^{-3}
{Day/night & thermal camera No.2, LiDAR}	3.58 10^{-3}	1.35 10^{-3}	1.13 10^{-3}	1.27 10^{-3}
{Day/night & thermal camera No.3, LiDAR}	3.58 10^{-3}	1.35 10^{-3}	1.13 10^{-3}	1.27 10^{-3}
{Day/night & thermal camera No.4, LiDAR}	3.58 10^{-3}	1.35 10^{-3}	1.13 10^{-3}	1.27 10^{-3}
{ECDIS, ECDIS (backup)}	2.77 10^{-3}	1.04 10^{-3}	8.78 10^{-4}	9.86 10^{-4}
{AI software, AI software (backup)}	2.73 10^{-3}	1.03 10^{-3}	8.64 10^{-4}	9.70 10^{-4}
{AI software (backup), Computer hardware}	1.10 10^{-3}	4.13 10^{-4}	3.47 10^{-4}	3.90 10^{-4}
{AI software, Computer hardware (backup)}	1.10 10^{-3}	4.13 10^{-4}	3.47 10^{-4}	3.90 10^{-4}
{RADAR, AIS}	5.04 10^{-4}	1.89 10^{-4}	1.59 10^{-4}	1.79 10^{-4}
{Computer hardware, Computer hardware (backup)}	4.41 10^{-4}	1.66 10^{-4}	1.40 10^{-4}	1.57 10^{-4}
{Radio system, LTE system}	3.26 10^{-4}	1.23 10^{-4}	1.03 10^{-4}	1.16 10^{-4}

monitoring and health assessment systems and/or alternative power plants with higher reliability (Tsoumpris and Theotokatos, 2022).

Finally, it should be mentioned that the component that exhibits the most considerable uncertainty in terms of its MTBF data is the AI software, due to the scanty of operational and accident data in similar systems (Wu et al., 2020). However, what is certain is that the AI software does fail (Yampolskiy and Spellchecker, 2016) but in a different way than humans do with potentially more severe consequences (Hecker et al., 2018), such as false object recognition due to incomplete training data set.

5. Conclusions

In this study, a methodology was developed to conduct the risk-informed Collision Avoidance System (CAS) design for MASSs. COLREG rules and SOLAS regulations/Chapter V were reviewed to identify functional and system requirements for the CAS. A baseline CAS configuration was developed by considering components that satisfy the identified requirements. The baseline CAS configuration was developed into a FT diagram by defining the failure of the CAS as the Top Event and embedding the Basic Events with relevant Mean Time Between Failure (MTBF) data. A case study of a Short Sea Shipping cargo ship that operates autonomously during the en route phase for 730 h was considered, and four operating modes were customised based on various weather and illumination conditions. Quantitative FTA was conducted to derive pertinent risk metrics and criticality analysis was conducted to identify the most critical components and weak design points. Finally, risk-reducing measures were recommended to develop a risk-informed CAS reconfiguration and their effectiveness in reducing the risk metrics was discussed. The main findings of this study are summarised as follows.

a. The developed FT diagram provided a robust representation of the failure of the CAS with reasonable MTBF data that enabled the accurate identification of the most critical components, failure mechanisms, and recommendation of cost-effective risk-reducing measures without the need of sensitivity analysis during its early design phase.
b. The CAS operating in adverse weather and daylight illumination condition (mode 3) exhibited the highest probability of failure, reaching up to 32% when operated for 730 h. The most critical components and failure mechanisms were related to the Intention Communication System (ICS) and Situation Awareness System (SAS), mainly the echo sounder, current profiler, visibility & weather sensor, anemometer, microphone, LCD panels, navigational lights, and speaker.
c. Identical or functional redundancy as a risk-reducing measure to the relatively inexpensive but critical components of the ICS and SAS was found to be effective in reducing the probability of failure of the CAS operating in mode 3 up to 91%.
d. The propulsion & steering system was found to be the most critical component in the risk-informed CAS reconfiguration, therefore indicating the need of intelligent monitoring and health assessment systems and/or alternative power plants as an effective risk-reducing measure.

The limitations of this study are associated with the currently non-

Table 11
Probability of failures of the TE and IEs and percentage contributions of each IE to the TE of the risk-informed CAS reconfiguration compared to the baseline CAS configuration in mode 3.

Event		Probability of failure at 730 h			
		Baseline CAS configuration in mode 3		Risk-informed CAS reconfiguration in mode 3	
TE	CAS failure	3.18 10^{-1}		2.84 10^{-2}	
IE	SAS failure	7.61 10^{-2}	23.93%	4.55 10^{-3}	16.01%
	DMS failure	6.36 10^{-4}	0.20%	6.36 10^{-4}	2.24%
	ICS failure	2.48 10^{-1}	78.12%	6.23 10^{-3}	21.94%
	AES failure	1.72 10^{-2}	5.41%	1.72 10^{-2}	60.61%

Table 12
Importance measures of the BEs of the risk-informed CAS reconfiguration in mode 3.

BE	I^B	I^{FV} or I^{CR}	BE	I^B	I^{FV} or I^{CR}
Propulsion & steering system	1.00	5.99 10^{-1}	Day/night & thermal camera No.2	1.21 10^{-2}	1.49 10^{-2}
LiDAR	1.42 10^{-1}	5.97 10^{-2}	Day/night & thermal camera No.3	1.21 10^{-2}	1.49 10^{-2}
Echo sounder	3.58 10^{-2}	4.47 10^{-2}	Day/night & thermal camera No.4	1.21 10^{-2}	1.49 10^{-2}
Echo sounder (backup)	3.58 10^{-2}	4.47 10^{-2}	ECDIS	1.82 10^{-2}	1.16 10^{-2}
GNSS	4.46 10^{-2}	2.50 10^{-2}	ECDIS (backup)	1.82 10^{-2}	1.16 10^{-2}
INS	1.61 10^{-2}	2.50 10^{-2}	Microphone	1.81 10^{-2}	1.14 10^{-2}
Stern light	2.40 10^{-2}	2.01 10^{-2}	Microphone (backup)	1.81 10^{-2}	1.14 10^{-2}
Stern light (backup)	2.40 10^{-2}	2.01 10^{-2}	Computer hardware	2.54 10^{-2}	6.42 10^{-3}
Masthead light No.1	2.40 10^{-2}	2.01 10^{-2}	Computer hardware (backup)	2.54 10^{-2}	6.42 10^{-3}
Masthead light No.1 (backup)	2.40 10^{-2}	2.01 10^{-2}	Visibility & weather sensor	1.28 10^{-2}	5.69 10^{-3}
Masthead light No.2	2.40 10^{-2}	2.01 10^{-2}	Visibility & weather sensor (backup)	1.28 10^{-2}	5.69 10^{-3}
Masthead light No.2 (backup)	2.40 10^{-2}	2.01 10^{-2}	LCD panel No.1	1.04 10^{-2}	3.74 10^{-3}
Starboard-side light	2.40 10^{-2}	2.01 10^{-2}	LCD panel No.1 (backup)	1.04 10^{-2}	3.74 10^{-3}
Starboard-side light (backup)	2.40 10^{-2}	2.01 10^{-2}	LCD panel No.2	1.04 10^{-2}	3.74 10^{-3}
Port-side light	2.40 10^{-2}	2.01 10^{-2}	LCD panel No.2 (backup)	1.04 10^{-2}	3.74 10^{-3}
Port-side light (backup)	2.40 10^{-2}	2.01 10^{-2}	LCD panel No.3	1.04 10^{-2}	3.74 10^{-3}
All-round light No.1	2.40 10^{-2}	2.01 10^{-2}	LCD panel No.3 (backup)	1.04 10^{-2}	3.74 10^{-3}
All-round light No.1 (backup)	2.40 10^{-2}	2.01 10^{-2}	LCD panel No.4	1.04 10^{-2}	3.74 10^{-3}
All-round light No.2	2.40 10^{-2}	2.01 10^{-2}	LCD panel No.4 (backup)	1.04 10^{-2}	3.74 10^{-3}
All-round light No.2 (backup)	2.40 10^{-2}	2.01 10^{-2}	AIS	8.30 10^{-3}	2.10 10^{-3}
All-round light No.3	2.40 10^{-2}	2.01 10^{-2}	RADAR	7.27 10^{-3}	2.10 10^{-3}
All-round light No.3 (backup)	2.40 10^{-2}	2.01 10^{-2}	LTE system	1.45 10^{-2}	1.36 10^{-3}
All-round light No.4	2.40 10^{-2}	2.01 10^{-2}	Radio system	2.70 10^{-3}	1.36 10^{-3}
All-round light No.4 (backup)	2.40 10^{-2}	2.01 10^{-2}	Anemometer	5.54 10^{-3}	1.07 10^{-3}
All-round light No.5	2.40 10^{-2}	2.01 10^{-2}	Anemometer (backup)	5.54 10^{-3}	1.07 10^{-3}
All-round light No.5 (backup)	2.40 10^{-2}	2.01 10^{-2}	Current profiler	3.24 10^{-3}	3.65 10^{-4}
AI software	2.54 10^{-2}	2.09 10^{-2}	Current profiler (backup)	3.24 10^{-3}	3.65 10^{-4}
AI software (backup)	2.54 10^{-2}	1.60 10^{-2}	Speaker	4.87 10^{-4}	8.23 10^{-6}
Day/night & thermal camera No.1	1.21 10^{-2}	1.49 10^{-2}	Speaker (backup)	4.87 10^{-4}	8.23 10^{-6}

existent regulatory instruments for MASSs, the uncertainty of MTBF data, especially of the AI software, and the lack of acceptable safety thresholds for MASS systems. Future studies entail the consideration of additional systems, such as cyber-security systems, and the investigation of specific accident scenarios. Nonetheless, this study provides a way forward to conduct risk-informed CAS design, hence support the MASSs safety enhancement.

Table 13
Probability of failures of the MCSs of the risk-informed CAS reconfiguration in mode 3.

MCS	Probability of failure
{Propulsion & steering system}	1.72 10^{-2}
{Echo sounder, Echo sounder (backup)}	1.29 10^{-3}
{INS, GNSS}	7.18 10^{-4}
{Stern light, Stern light (backup)}	5.78 10^{-4}
{Masthead light No.1, Masthead light No.1(backup)}	5.78 10^{-4}
{Masthead light No.2, Masthead light No.2 (backup)}	5.78 10^{-4}
{Starboard-side light, Starboard-side light (backup)}	5.78 10^{-4}
{Port-side light, Port-side light (backup)}	5.78 10^{-4}
{All-round light No.1, All-round light No.1 (backup)}	5.78 10^{-4}
{All-round light No.2, All-round light No.2 (backup))}	5.78 10^{-4}
{All-round light No.3, All-round light No.3 (backup)}	5.78 10^{-4}
{All-round light No.4, All-round light No.4 (backup)}	5.78 10^{-4}
{All-round light No.5, All-round light No.5 (backup)}	5.78 10^{-4}
{Day/night & thermal camera No.1, LiDAR}	4.29 10^{-4}
{Day/night & thermal camera No.2, LiDAR}	4.29 10^{-4}
{Day/night & thermal camera No.3, LiDAR}	4.29 10^{-4}
{Day/night & thermal camera No.4, LiDAR}	4.29 10^{-4}
{ECDIS, ECDIS (backup)}	3.32 10^{-4}
{AI software, AI software (backup)}	3.27 10^{-4}
{Microphone, Microphone (backup)}	3.27 10^{-4}
{Visibility & weather sensor, Visibility & weather sensor (backup)}	1.64 10^{-4}
{AI software (backup), Computer hardware}	1.32 10^{-4}
{AI software, Computer hardware (backup)}	1.32 10^{-4}
{LCD panel No.1, LCD panel No.1 (backup)}	1.08 10^{-4}
{LCD panel No.2, LCD panel No.2 (backup)}	1.08 10^{-4}
{LCD panel No.3, LCD panel No.3 (backup)}	1.08 10^{-4}
{LCD panel No.4, LCD panel No.4 (backup)}	1.08 10^{-4}
{RADAR, AIS}	6.04 10^{-5}
{Computer hardware, Computer hardware (backup)}	5.29 10^{-5}
{Radio system, LTE system}	3.91 10^{-5}
{Anemometer, Anemometer (backup)}	3.07 10^{-5}
{Current profiler, Current profiler (backup)}	1.05 10^{-5}
{Speaker, Speaker (backup)}	2.37 10^{-7}

CRediT authorship contribution statement

Paul Lee: Conceptualization, Methodology, Software, Validation, Visualization, Resources, Writing – original draft, Writing – review & editing. **Gerasimos Theotokatos:** Conceptualization, Methodology, Validation, Supervision, Visualization, Writing – review & editing. **Evangelos Boulougouris:** Conceptualization, Supervision, Writing – review & editing. **Victor Bolbot:** Conceptualization, Resources, Supervision, Writing – review & editing.

Declaration of competing interest

The authors declare that they have no known competing financial interests or personal relationships that could have appeared to influence the work reported in this paper.

Data availability

No data was used for the research described in the article.

Acknowledgements

The study was carried out in the framework of the AUTOSHIP project, which is funded by the European Union's Horizon 2020 research and innovation programme under agreement No 815012. The authors affiliated with the MSRC greatly acknowledge the funding from DNV AS and RCCL for the MSRC establishment and operation. The opinions expressed herein are those of the authors and should not be construed to reflect the views of EU, DNV AS, and RCCL.

Appendix A

Table A1
Abbreviation list

Abbreviation	Full form
AES	Action Execution system
AI	Artificial Intelligence
AIS	Automatic Identification System
BBN	Bayesian Belief Network
BE	Basic Event
BN	Bayesian Networks
CAS	Collision Avoidance System
COLREG	Convention on the International REGulations for Preventing COLlisions at Sea
DMS	Decision Making System
ECDIS	Electronic Chart Display and Information System
FT	Fault Tree
FTA	Fault Tree Analysis
GNSS	Global Navigation Satellite System
HCL	Hybrid Causal Logic
I^B	Birnbaum Importance measure
I^{CR}	Criticality Importance measure
I^{FV}	Fussell-Vesely Importance measure
ICS	Intention Communication system
IE	Intermediate Event
IMO	International Maritime Organisation
INS	Inertial Navigation System
LCD	Liquid Crystal Display
LiDAR	LIght Detection And Ranging
LTE	Long Term Evolution
MASS	Maritime Autonomous Surface Ships
MCS	Minimal Cut Set
MTBF	Mean Time Between Failure
OS	Own Ship
RADAR	RAdio Detection And Ranging
SAS	Situation Awareness System
SOLAS	International Convention for the Safety Of Life At Sea
SSS	Short Sea Shipping
STPA	Systems-Theoretic Process Analysis
SWIFT	Structured What-IF Technique
TE	Top Event
TS	Target Ship

Appendix B

This appendix provides the results of the FTA for the baseline CAS configuration in modes 1–4 and for the risk-informed CAS reconfiguration in mode 3 using the PTC Windchill (PTC, 2021) environment.

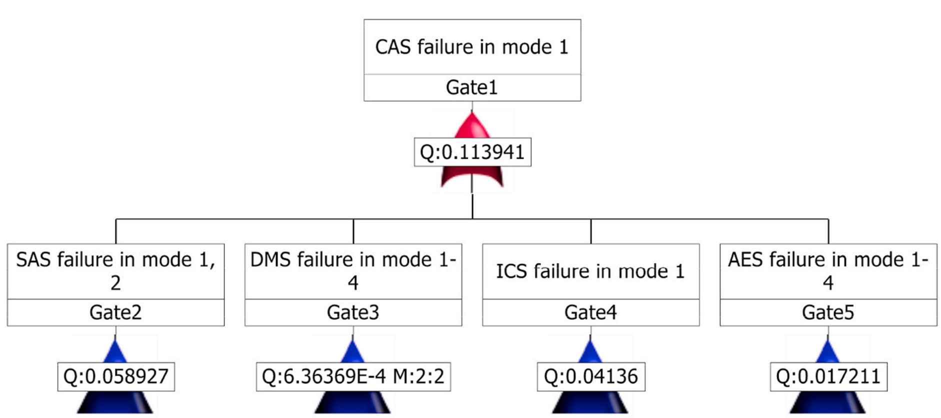

Fig. B.1. Probability of failure of the baseline CAS configuration in mode 1.

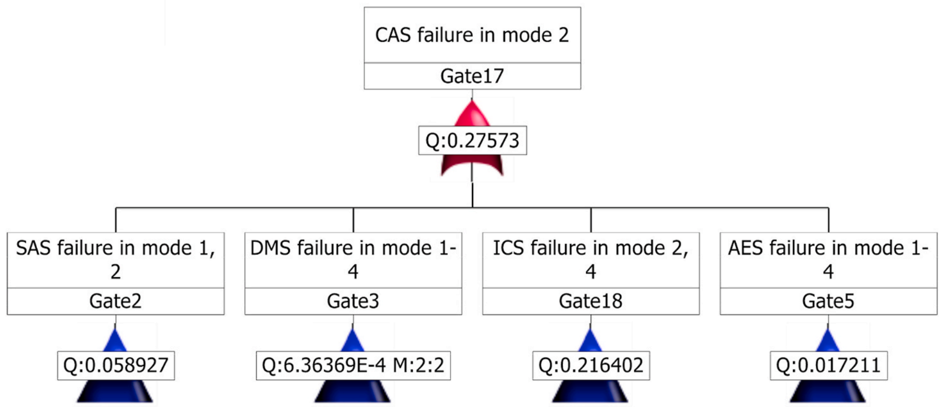

Fig. B.2. Probability of failure of the baseline CAS configuration in mode 2.

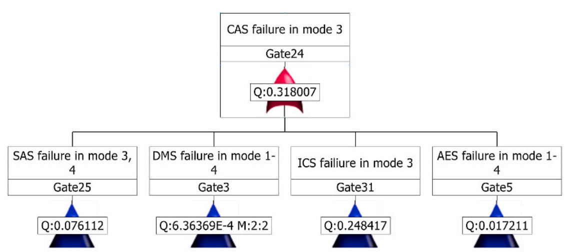

Fig. B.3. Probability of failure of the baseline CAS configuration in mode 3.

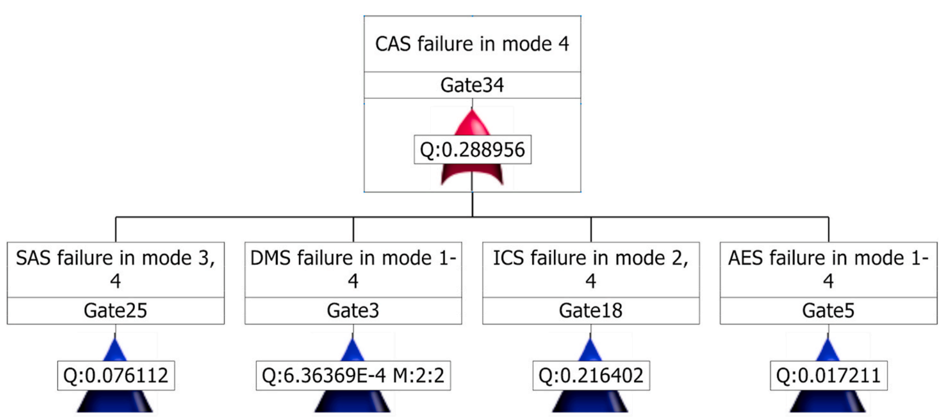

Fig. B.4. Probability of failure of the baseline CAS configuration in mode 4.

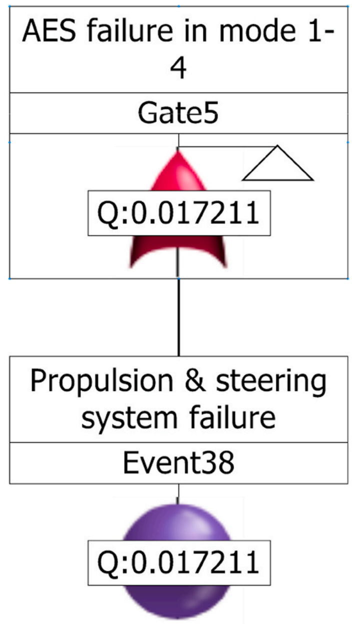

Fig. B.5. Probability of failure of the AES in the baseline CAS configuration in modes 1–4.

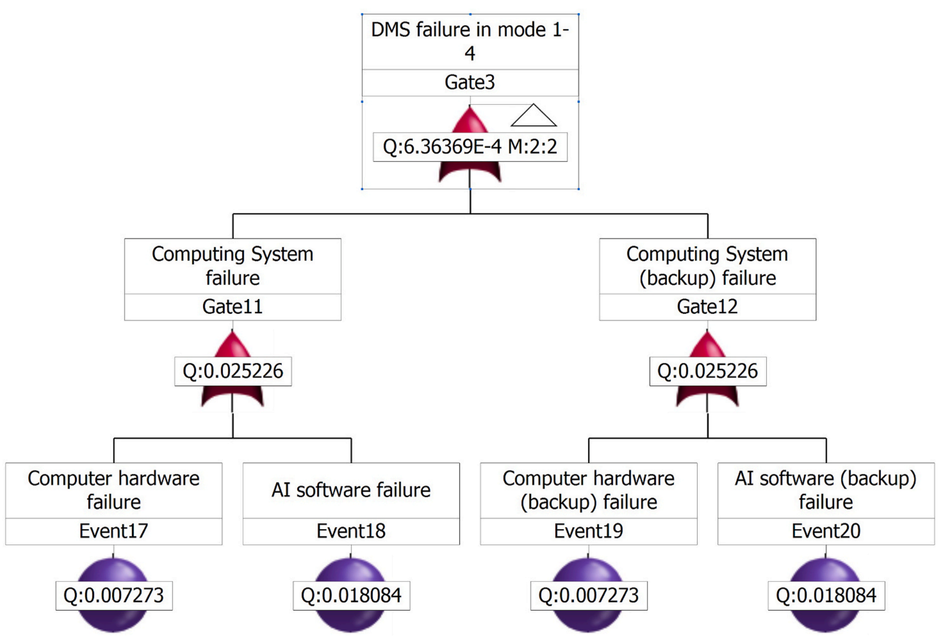

Fig. B.6. Probability of failure of the DMS in the baseline CAS configuration in modes 1–4.

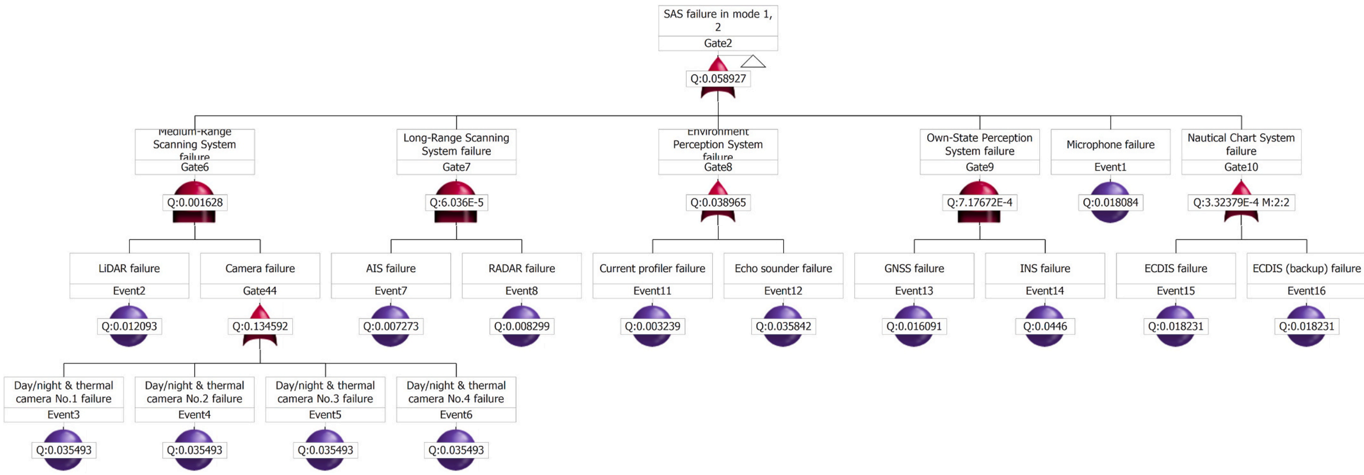

Fig. B.7. Probability of failure of the SAS in the baseline CAS configuration in modes 1–2.

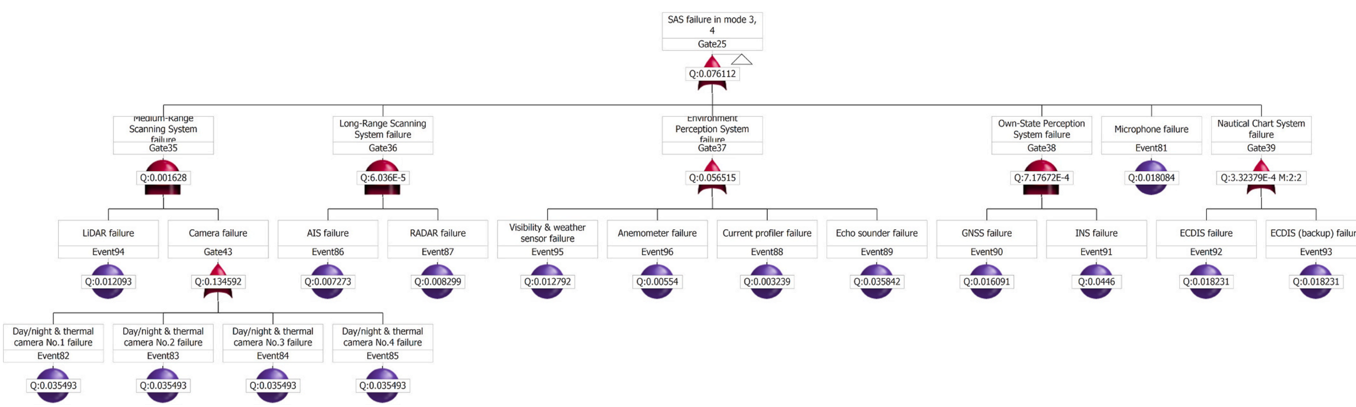

Fig. B.8. Probability of failure of the SAS in the baseline CAS configuration in modes 3–4.

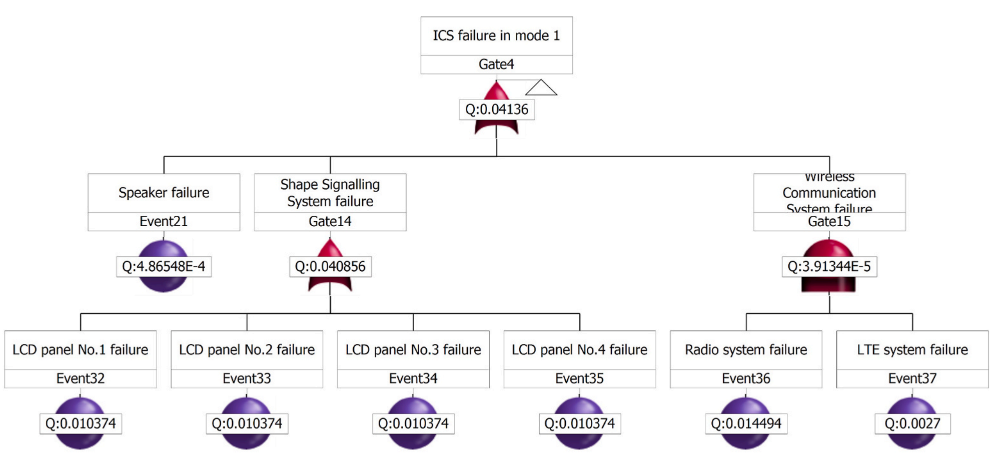

Fig. B.9. Probability of failure of the ICS in the baseline CAS configuration in mode 1.

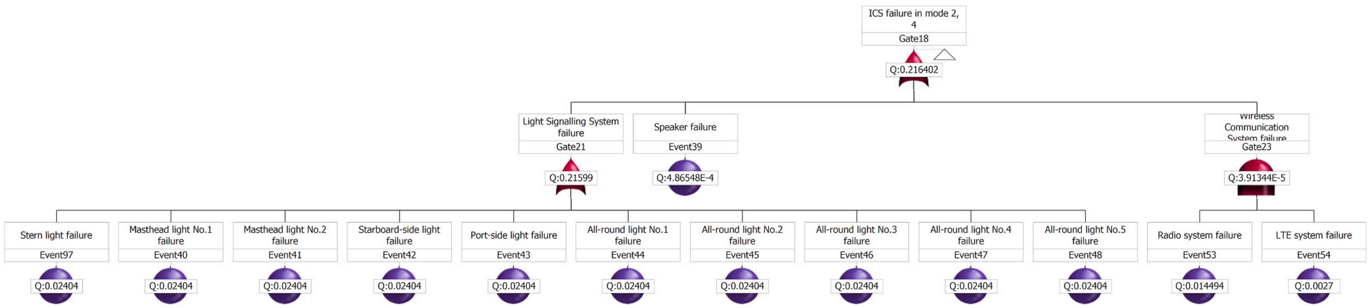

Fig. B.10. Probability of failure of the ICS in the baseline CAS configuration in modes 2 and 4.

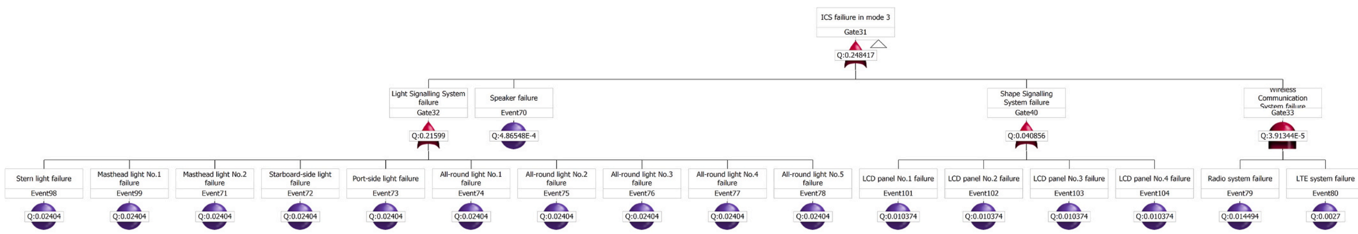

Fig. B.11. Probability of failure of the ICS in the baseline CAS configuration in mode 3.

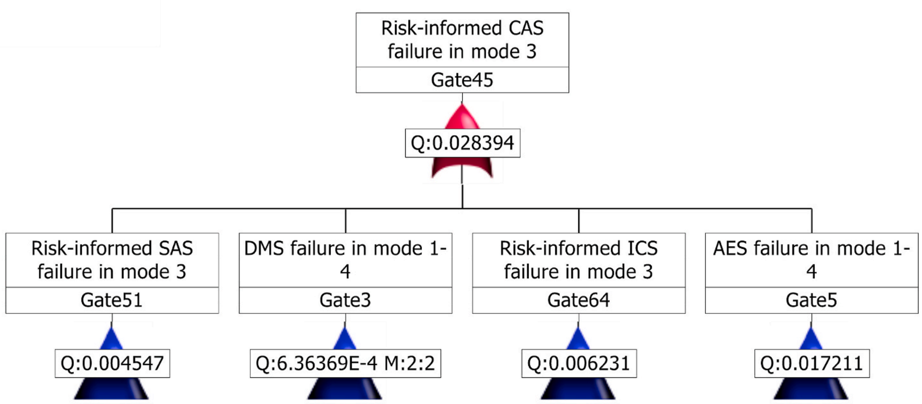

Fig. B.12. Probability of failure of the risk-informed CAS reconfiguration in mode 3.

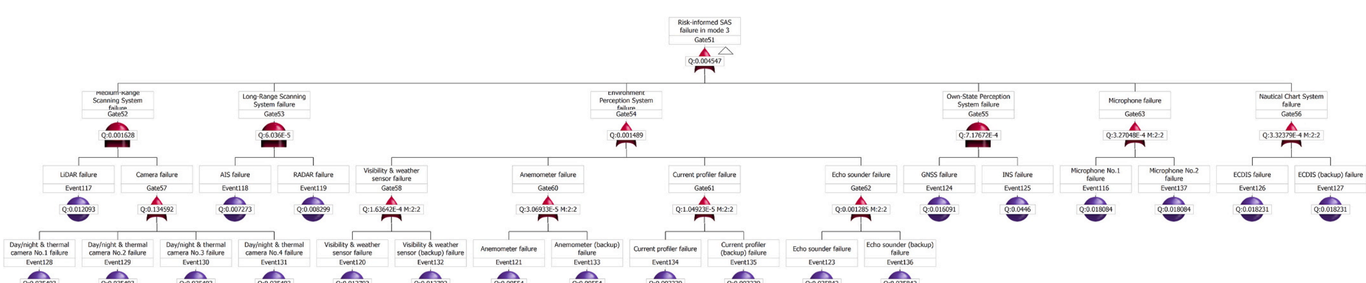

Fig. B.13. Probability of failure of the SAS in the risk-informed CAS reconfiguration in mode 3.

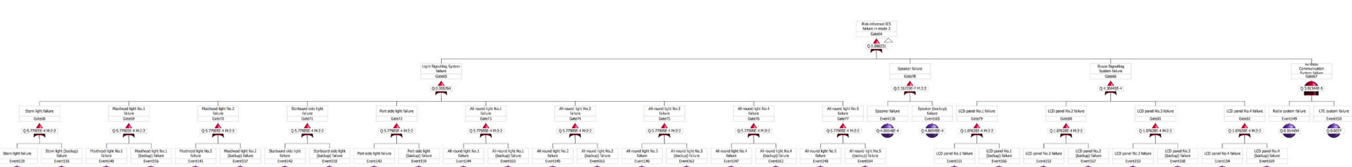

Fig. B.14. Probability of failure of the ICS in the risk-informed CAS reconfiguration in mode 3.

References

Abaei, M.M., Hekkenberg, R., BahooToroody, A., 2021. A multinomial process tree for reliability assessment of machinery in autonomous ships. Reliab. Eng. Syst. Saf. 210, 107484.
Abduljabbar, R., Dia, H., Liyanage, S., Bagloee, S.A., 2019. Applications of artificial intelligence in transport: an overview. Sustainability 11 (1), 189.
Aiello, G., Giallanza, A., Mascarella, G., 2020. Towards Shipping 4.0. A preliminary gap analysis. Procedia Manuf. 42, 24–29.
Ametller, X., 2015. Freight transport using short sea shipping. J. Shipp. Ocean Eng. 5, 143–150.
Aven, T., 1985. Reliability/availability evaluations of coherent systems based on minimal cut sets. Reliab. Eng. 13 (2), 93–104.
Aven, T., 2015. Risk Analysis. John Wiley & Sons.
Bäckström, O., Butkova, Y., Hermanns, H., Krčál, J., Krčál, P., 2016. Effective Static and Dynamic Fault Tree Analysis, International Conference on Computer Safety, Reliability, and Security. Springer, pp. 266–280.
Banda, O.A.V., Kannos, S., Goerlandt, F., van Gelder, P.H., Bergström, M., Kujala, P., 2019. A systemic hazard analysis and management process for the concept design phase of an autonomous vessel. Reliab. Eng. Syst. Saf. 191, 106584.
Banda, O.V., Kujala, P., Goerlandt, F., Bergström, M., Ahola, M., van Gelder, P., Sonninen, S., 2018. The Need for Systematic and Systemic Safety Management for Autonomous Vessels. Marine Design XIII. CRC Press, pp. 853–859.
Bjornland, D., 1993. The Importance of Short Sea Shipping in European Transport. ECTM, Short Sea Shipping (Economic Research Center).
Bobbio, A., Raiteri, D.C., 2004. Parametric Fault Trees with Dynamic Gates and Repair Boxes, Annual Symposium Reliability and Maintainability, 2004-RAMS. IEEE, pp. 459–465.
Bolbot, V., Theotokatos, G., Boulougouris, E., Vassalos, D., 2020. A novel cyber-risk assessment method for ship systems. Saf. Sci. 131, 104908.
Brocken, E., 2016. Improving the Reliability of Ship Machinery: A Step towards Unmanned Shipping.
Chang, C.-H., Kontovas, C., Yu, Q., Yang, Z., 2021. Risk assessment of the operations of maritime autonomous surface ships. Reliab. Eng. Syst. Saf. 207, 107324.
Changcong, Z., Qi, C., Chunping, Z., Haodong, Z., Zhuangke, S., 2021. Fault tree analysis of an aircraft flap system based on a non-probability model. J. Tsinghua Univ. (Sci. Technol.) 61 (6), 636–642.
Cheok, M.C., Parry, G.W., Sherry, R.R., 1998. Use of importance measures in risk-informed regulatory applications. Reliab. Eng. Syst. Saf. 60 (3), 213–226.
Chou, C.-C., Wang, C.-N., Hsu, H.-P., 2022. A novel quantitative and qualitative model for forecasting the navigational risks of Maritime Autonomous Surface Ships. Ocean. Eng. 248, 110852.
DatCon, 2022. Long and Medium Range - Modular Multi Sensor System.
DNV, G., 2018. Autonomous and Remotely Operated Ships. DNVGL-CG-0264, 2018-2009.
Dugan, J.B., Bavuso, S.J., Boyd, M.A., 1990. Fault trees and sequence dependencies. In: Annual Proceedings on Reliability and Maintainability Symposium, pp. 286–293. IEEE.
Dugan, J.B., Bavuso, S.J., Boyd, M.A., 1992. Dynamic fault-tree models for fault-tolerant computer systems. IEEE Trans. Reliab. 41 (3), 363–377.
EMSA, 2021. Annual Overview of Marine Casualties and Incidents 2021.
Eriksen, S., Utne, I.B., Lützen, M., 2021. An RCM approach for assessing reliability challenges and maintenance needs of unmanned cargo ships. Reliab. Eng. Syst. Saf. 210, 107550.
Gao, T., Liu, M., Qu, H.-Y., Ji, H.-J., Jing, J., 2021. Reliability design of aerospace secondary power supply based on fault tree analysis. In: IOP Conference Series: Materials Science and Engineering, 042059. IOP Publishing.
Goerlandt, F., Kujala, P., 2011. Traffic simulation based ship collision probability modeling. Reliab. Eng. Syst. Saf. 96 (1), 91–107.
Guo, C., Haugen, S., Utne, I.B., 2021. Risk assessment of collisions of an autonomous passenger ferry. Proc. Inst. Mech. Eng. O J. Risk Reliab. 1748006X211050714.
Hansen, J.F., Wendt, F., 2015. History and state of the art in commercial electric ship propulsion, integrated power systems, and future trends. Proc. IEEE 103 (12), 2229–2242.
Hecker, S., Dai, D., Van Gool, L., 2018. Failure Prediction for Autonomous Driving, 2018 IEEE Intelligent Vehicles Symposium (IV). IEEE, pp. 1792–1799.
Hokstad, P., Utne, I.B., Vatn, J., 2012. Risk and Vulnerability Analysis of Critical Infrastructures, Risk and Interdependencies in Critical Infrastructures. Springer, pp. 23–33.
IEC, 2006. Fault Tree Analysis (FTA).
IMO, 2018a. COLREG: Convention on the International Regulations for Preventing Collisions at Sea, 1972. Consolidated Edition 2018 (International Maritime Organization).
IMO, 2018b. IMO Takes First Steps to Address Autonomous Ships.
IMO, 2019. Interim Guidelines for MASS Trials.
IMO, 2020. SOLAS: Consolidated Edition 2020. IMO Publishing Group.
IMO, 2021a. Autonomous Shipping.
IMO, 2021b. Outcome of the Regulatory Scoping Exercise for the Use of Maritime Autonomous Surface Ships (MASS).
IMO, I., 2002. Guidelines for Formal Safety Assessment (FSA) for Use in the IMO Rule-Making Process, vol. 1023. MSC/Circ.. MEPC/Circ. 392, Ref T1/3.02, T5/1.01.
James, A.T., Gandhi, O., Deshmukh, S., 2018. Fault diagnosis of automobile systems using fault tree based on digraph modeling. Int. J. Syst. Assurance Eng. Manage. 9 (2), 494–508.
Jovanović, I., Vladimir, N., Perčić, M., Koričan, M., 2022. The feasibility of autonomous low-emission ro-ro passenger shipping in the Adriatic Sea. Ocean. Eng. 247, 110712.
Krasich, M., 2009. How to estimate and use MTTF/MTBF would the real MTBF please stand up?. In: 2009 Annual Reliability and Maintainability Symposium, pp. 353–359. IEEE.
Kretschmann, L., Rødseth, Ø., Tjora, Å., Fuller, B., Noble, H., Horahan, J., 2015. In: Maritime Unmanned Navigation through Intelligence in Networks – D9.3: Qualitative Assessment, MUNIN Project Report.
Kumar, U.D., Knezevic, J., Crocker, J., 1999. Maintenance free operating period–an alternative measure to MTBF and failure rate for specifying reliability? Reliab. Eng. Syst. Saf. 64 (1), 127–131.
MicroStep-MIS, 2022a. Visibility and Present Weather Sensor: VPF-730 Series.
MicroStep-MIS, 2022b. Windsonic 75 Anemometer.
Misra, K.B., 2008. Handbook of Performability Engineering. Springer.
Muhammad, M., Abd Majid, M.A., Ibrahim, N.A., 2010. A Case Study of Reliability Assessment for Centrifugal Pumps in a Petrochemical Plant, Engineering Asset Lifecycle Management. Springer, pp. 398–404.
Murawski, L., 2018. Thermal interaction between main engine body and ship hull. Ocean. Eng. 147, 107–120.
PTC, 2021. Windchill PLM Software.
Purba, J.H., 2014. A fuzzy-based reliability approach to evaluate basic events of fault tree analysis for nuclear power plant probabilistic safety assessment. Ann. Nucl. Energy 70, 21–29.
Rausand, M., 2014. Reliability of Safety-Critical Systems: Theory and Applications. John Wiley & Sons.
Rausand, M., Haugen, S., 2020. Risk Assessment: Theory, Methods, and Applications, second ed. John Wiley & Sons.
Rausand, M., Hoyland, A., 2003. System Reliability Theory: Models, Statistical Methods, and Applications. John Wiley & Sons.
Rødseth, Ø., Tjora, A., 2014. A risk based approach to the design of unmanned ship control systems. Proceeding Conf. Marit. Technol. 153–162.
Rødseth, Ø.J., Burmeister, H.-C., 2015. Risk assessment for an unmanned merchant ship. TransNav: Int. J. Marine Navigate. Safety Sea Transport. 9 (3), 357–364.
Rødseth, Ø.J., Faivre, J., Hjørunges, S., Andersen, P., Bolbot, V., Pauwelyn, A.-S., Wennersberg, L., 2021. AUTOSHIP Deliverable D3.1: Autonomous Ship Design Standards.
Rødseth, Ø.J., Perera, L.P., Mo, B., 2016. Big Data in Shipping-Challenges and Opportunities.
Ruijters, E., Stoelinga, M., 2015. Fault tree analysis: a survey of the state-of-the-art in modeling, analysis and tools. Comput. Sci. Rev. 15, 29–62.
Sharma, P., Singh, A., 2015. Overview of Fault Tree analysis. Int. J. Eng. Res. Technol. 4 (3), 337–340.
Singh, K., Kaushik, M., Kumar, M., 2022. Integrating α-cut interval based fuzzy fault tree analysis with Bayesian network for criticality analysis of submarine pipeline leakage: a novel approach. Process Saf. Environ. Protect. 166, 189–201.
Sonardyne, 2022. Doppler Velocity Log with Integrated ADCP - Syrinx DVL.
Statheros, T., Howells, G., Maier, K.M., 2008. Autonomous ship collision avoidance navigation concepts, technologies and techniques. J. Navig. 61 (1), 129–142.
Tanaka, H., Fan, L., Lai, F., Toguchi, K., 1983. Fault-tree analysis by fuzzy probability. IEEE Trans. Reliab. 32 (5), 453–457.
Teledynemarine, 2021. MK31 INS.
Thieme, C.A., Guo, C., Utne, I.B., Haugen, S., 2019. Preliminary hazard analysis of a small harbor passenger ferry–results, challenges and further work. J. Phys. Conf. Ser., 012024. IOP Publishing.
Thieme, C.A., Utne, I.B., 2017. A risk model for autonomous marine systems and operation focusing on human–autonomy collaboration. Proc. Inst. Mech. Eng. O J. Risk Reliab. 231 (4), 446–464.
Torell, W., Avelar, V., 2004. Mean time between failure: explanation and standards. White Paper. 78, 6–7.
Tsoumpris, C., Theotokatos, G., 2022. Performance and reliability monitoring of ship hybrid power plants. J. ETA Maritime Sci. 10 (1), 29–38.
Ugurlu, H., Cicek, I., 2022. Analysis and assessment of ship collision accidents using Fault Tree and multiple correspondence analysis. Ocean. Eng. 245, 110514.
Utne, I.B., Rokseth, B., Sørensen, A.J., Vinnem, J.E., 2020. Towards supervisory risk control of autonomous ships. Reliab. Eng. Syst. Saf. 196, 106757.
Van Eck, N., Waltman, L., 2010. Software survey: VOSviewer, a computer program for bibliometric mapping. Scientometrics 84 (2), 523–538.
Veritas, B., 2019. NI641 Guidelines for Autonomous Shipping.
Wang, Y., Yanushkevich, S., Hou, M., Plataniotis, K., Coates, M., Gavrilova, M., Hu, Y., Karray, F., Leung, H., Mohammadi, A., 2020. A Tripartite Theory of Trustworthiness for Autonomous Systems, 2020 IEEE International Conference on Systems, Man, and Cybernetics (SMC), pp. 3375–3380. IEEE.
Wróbel, K., Krata, P., Montewka, J., 2019. Preliminary results of a system-theoretic assessment of maritime autonomous surface ships' safety. TransNav. Int. J. Marine Navigate. Safety Sea Transport. 13 (4).
Wróbel, K., Krata, P., Montewka, J., Hinz, T., 2016. Towards the development of a risk model for unmanned vessels design and operations. TransNav. Int. J. Marine Navigate. Safety Sea Transport. 10 (2).
Wróbel, K., Montewka, J., Kujala, P., 2017. Towards the assessment of potential impact of unmanned vessels on maritime transportation safety. Reliab. Eng. Syst. Saf. 165, 155–169.
Wróbel, K., Montewka, J., Kujala, P., 2018a. System-theoretic approach to safety of remotely-controlled merchant vessel. Ocean. Eng. 152, 334–345.
Wróbel, K., Montewka, J., Kujala, P., 2018b. Towards the development of a system-theoretic model for safety assessment of autonomous merchant vessels. Reliab. Eng. Syst. Saf. 178, 209–224.

Wu, Q., Wang, T., Diaconeasa, M.A., Mosleh, A., Wang, Y., 2020. A comparative assessment of collision risk of manned and unmanned vessels. J. Mar. Sci. Eng. 8 (11), 852.

Xiao, G., Li, Z., Li, T., 2007. Dependability estimation for non-Markov consecutive-k-out-of-n: F repairable systems by fast simulation. Reliab. Eng. Syst. Saf. 92 (3), 293–299.

Xing, L., Amari, S.V., 2008. Fault tree analysis. Handbook. Perform Eng. 595–620.

Xu, H., Li, G., Liu, J., 2013. Reliability Analysis of an Autonomous Underwater Vehicle Using Fault Tree, 2013 IEEE International Conference on Information and Automation (ICIA), pp. 1165–1170. IEEE.

Yampolskiy, R.V., Spellchecker, M., 2016. Artificial Intelligence Safety and Cybersecurity: A Timeline of AI Failures arXiv preprint arXiv:1610.07997.

Yuan, J., Long, Y., 2010. The Missile Flight Control System Reliability Analysis Based on Hybrid Fault Trees, 2010 2nd International Asia Conference on Informatics in Control, Automation and Robotics (CAR 2010). IEEE, pp. 158–160.

Zhang, D., Han, Z., Zhang, K., Zhang, J., Zhang, M., Zhang, F., 2022. Use of hybrid causal logic method for preliminary hazard analysis of maritime autonomous surface ships. J. Mar. Sci. Eng. 10 (6), 725.

Zhou, X., Liu, Z., Wu, Z., Wang, F., 2019. Quantitative processing of situation awareness for autonomous ships navigation. TransNav: Int. J. Marine Navigate. Safety Sea Transport. 13.